Environmental Science

AIMS Environmental Science, 13(2): 241–299.
DOI: 10.3934/environsci.2026010
Received: 13 November 2025
Revised: 04 February 2026
Accepted: 16 March 2026
Published: 25 March 2026

http://www.aimspress.com/journal/environmental

Review

A review on carbon-based materials for the adsorptive removal of per- and polyfluoroalkyl substances from the environment

Josephine Baffoe[1,2], Eliasu Issaka[3,*] and Eric Danso-Boateng[4]

[1] School of Automotive and Traffic Engineering, Jiangsu University, Zhenjiang 212013, China
[2] School of Energy and Power Engineering, Jiangsu University, Zhenjiang 212013, China
[3] School of Architecture, Built Environment, Computing and Engineering, College of Engineering, Birmingham City University, Birmingham B4 7XG, United Kingdom
[4] School of Chemical and Process Engineering, University of Leeds, Leeds, LS2 9JT, United Kingdom

* **Correspondance:** Email: eliasu.issaka@mail.bcu.ac.uk.

Abstract: Per- and polyfluoroalkyl substances (PFAS) are hazardous, persistent, and widely used compounds that pose significant risks to human health and the environment. Urgent and effective techniques for removing PFAS from aquatic environments are needed. Carbon-based materials, including activated hydrochar (AHC), biochar (BC), graphene oxide (GO), carbon nanotubes (CNT), and granular activated carbon (GAC), have become valuable adsorbents due to their high surface area, porosity, and adaptable properties. This review comprehensively discusses these five carbon-based materials, outlining their synthesis and applications for PFAS adsorption. Additionally, the review explains the underlying mechanisms of adsorption and the models used, such as the Langmuir and Freundlich isotherms, as well as Pseudo-first- and second-order kinetic models. Furthermore, the study contributes to the current body of knowledge by suggesting and explaining practical modification options tailored to capture low-molecular-weight, short-chain PFAS (S-C PFAS). By moving the focus from classical hydrophobic partitioning to electrostatic-driven design, revealing cationic functionalisation and metal oxide doping as critical approaches for overcoming short-chain compounds' water mobility. Functional group analysis, linkage of molecular structure to adsorption potential, comparison of carbon-based materials for adsorption, and practical cases and techniques for regeneration and reuse of the five carbon-based materials have all been discussed. The review paper also explores potential research directions to improve material design, cost-effectiveness, and sustainability, considering current limitations of each carbon-based adsorbent. To conclude, it references recent publications to examine the various applications of these materials for removing

PFAS from the environment. This review aims to assist researchers and academics working towards reducing PFAS contamination.

Keywords: PFAS; carbon-based materials; activated carbon (AC); carbon nanotubes (CNTs); Graphene oxide (GO)

1. Introduction

Per- and polyfluoroalkyl substances (PFAS) are a vast group of synthetic compounds that are widely employed in industrial and consumer applications due to their exceptional resistance to heat, water, and oil [1,2]. However, these same qualities make PFAS extremely persistent in the environment, earning them the epithet "forever chemicals." Their extensive usage and environmental stability have resulted in worldwide pollution of water supplies, creating serious concerns about their negative impact on human health and ecosystems [2]. PFAS exposure has been related to several health hazards, including immune system suppression, developmental difficulties, and an increased risk of cancer [1,3]. Because PFAS are chemically stable and resistant to degradation, conventional water treatment technologies are frequently inefficient at eliminating them [4]. As a result, improved treatment methods are needed to combat PFAS contamination in water systems. Carbon-based compounds, such as activated carbon (AC) [5], biochar (BC) [6], carbon nanotubes (CNT) [7], activated hydrochar (AHC) [8] and graphene oxide (GO) [9], stand out as some of the most promising PFAS removal methods. These materials have a large surface area, variable surface chemistry, and strong adsorptive characteristics [10], making them useful for removing PFAS from polluted water.

Adsorption employing a variety of adsorbents, particularly granular [11] and powdered activated carbon (AC) [5], carbonaceous additives, CNTs, and different polymeric materials, is one of the frequently used removal techniques [12]. Granular activated carbon (GAC) is a potential way to remove PFAS from drinking water. However, GAC filters frequently experience early PFAS breakthroughs because of competition between PFAS and natural organic matter (NOM) during sorption. Liu et al. [13] presented a study that looked at the possibilities of employing ozonation to improve GAC performance for PFAS removal. Three GACs were subjected to rapid small-scale column testing with either filtered or filtered and ozonated water. Ozonation's influence on GAC performance for NOM and PFAS removal was mostly determined by GAC characteristics. When ozonation was used, GACs with smaller micropore volumes performed better in terms of NOM and PFAS removal, approaching the performance of GACs with bigger micropore sizes. Furthermore, Yin et al. [14] synthesized, characterized and employed nano-$MgAl_2O_4$ modified CNTs as nano adsorbents to eliminate Perfluorooctanoic acid (PFOA) levels from drinking water and brackish groundwater at ppb (μg/L). Adsorption studies from ground and drinking water samples demonstrated that nano-MgAl2O4@CNTs is an effective nano-adsorbent for PFOA removal. Besides, Liu et al. [15] synthesised Fe-doped (R-Fe) and Cu-doped biochars (R-Cu) from reed straw BC. R-Fe had significantly greater perfluorobutanoic acid (PFBA) and perfluoropentanoic Acid (PFPeA) sorption capacities (25.81 and 43.59 mg g^{-1}, respectively) compared to R. R-Cu had PFBA and PFPeA with sorption capacities of 19.34 and 33.69 mg g^{-1}, respectively, which were 1.24 and 1.20 times greater. Furthermore, R-Fe and R-Cu outperformed previously reported BC in terms of PFBA and PFPeA sorption capacity. The BCs' exceptional PFAS sorption ability was due to R's extremely porous

structure, which supplied many adsorption sites. Ion-pair sorption, pore filling, and electrostatic interaction of Fe/Cu were the mechanisms of cationic groups on BC. Also, Miserli et al. [16] used sonication-solid phase extraction to identify fifteen PFAS in sludge and hydrochar (HC) substrates, which were then analysed using liquid chromatography-Orbitrap-Orbitrap-High Resolution mass spectroscopy/mass spectroscopy (LC-Orbitrap-High Resolution-MS/MS). The technique was completely verified and showed extremely strong linearity, recoveries ranging from 48 to 126 %, and low detection and quantification limits with increased uncertainty and accuracy below 32 % and 21.9 %, respectively.

PFAS in the environment have been extensively researched by several studies; including their sources [17], properties and fate [18]. Nonetheless, to the best of our knowledge, no publication has thoroughly assessed the recent research on the use of adsorption as an integral process for the removal of PFAS, encompassing the sorption properties of PFASs for a myriad of adsorbent materials. This current review paper is presented for these and other reasons as an addition to the body of knowledge on the state-of-the-art development of PFAS. Herein, this research begins by discussing a myriad of adsorbents and their sorption process for PFAS removal. The characteristic properties and synthesis processes of GAC-activated hydrochar (AHC), BC, CNTs, and GO for the application in the removal of PFASs are elucidated. Furthermore, this study elucidates adsorption mechanisms as well as a discussion of adsorption models (Langmuir isotherm and the Freundlich isotherm model) and kinetic models (Pseudo-first and second-order adsorption kinetic model). Besides, the review expands the existing body of knowledge by proposing and detailing actionable modification strategies specifically designed to capture low-molecular-weight, short-chain PFAS. By shifting the focus from traditional hydrophobic partitioning (which is effective for long-chain species) to electrostatic-driven design, the manuscript identifies cationic functionalisation and metal oxide doping as essential routes for overcoming the water mobility of short-chain compounds. The study concludes by discussing the several challenges associated with using these adsorbents to remove PFASSs, as well as the current and potential future research avenues for enhancing their effectiveness, stability, and environmental friendliness. In addition to introducing PFASs as an essential contaminant, the goal is to give researchers a concise and thorough summary of the present status of PFAS adsorption research, which will serve as a roadmap for both ongoing and future research.

2. Per- and polyfluoroalkyl substances (PFAS) in the environment

A myriad of studies have recently discussed the persistence of PFAS in the environment. To not present existing information, this section only summarises vital information that, to the best of our knowledge, has not been presented elsewhere. Reports on the sources, classes, properties, fate, exposure pathways and toxicological implications of PFAS to human health are presented herein.

2.1. Sources, classes, properties, fate, exposure pathways and toxicological implications of PFAS in the environment.

2.1.1. Sources of PFAS in the environment

PFAS in the environment come from both direct and diffuse sources, demonstrating their extensive industrial value and chemical durability (Figure 1) [19]. Historically, fluorochemical industrial processes have been key contributors, with industries producing or processing PFAS

frequently releasing these pollutants through wastewater discharges, air emissions, and poor waste management. These industrial sites, which include operations that produce coatings, lubricants, plastics, and surfactants, have contaminated the surrounding soil, water, and sediments [20]. Besides, aqueous film-forming foams (AFFF) are a particularly infamous source of PFAS, as they are widely employed in firefighting activities at military bases, airports, and industrial fire training locations [21]. When these foams are used to extinguish fires, particularly those containing hydrocarbons, they can seep into soils and move into surface and groundwater systems, causing long-term contamination that can last decades owing to the refractory nature of PFAS chemicals. PFAS residues from AFFF deployment have been detected in drinking water sources around defunct and active military sites and airports across the world [22].

Furthermore, municipal waste sources also contribute significantly to environmental PFAS pollution. Everyday consumer items, such as stain-resistant fabrics, nonstick cookware, water-repellent clothes, food packaging, and some personal care products, frequently include PFAS to provide chemical resistance. PFAS enter wastewater systems from routine usage, cleaning, or disposal of these products. Most traditional wastewater treatment plants are not designed to completely remove PFAS, resulting in its release into surface waterways or buildup in sewage sludge, which can subsequently be used as fertiliser on agricultural land. Because these compounds are not easily destroyed, they can slowly leak into groundwater or be discharged back into the environment via agricultural runoff.

Landfills accepting PFAS-laden municipal solid waste are yet another source of environmental pollution. Leachate from these locations, which contain PFAS from decaying commercial and home objects, might penetrate groundwater or be transferred elsewhere for treatment, where removal is frequently poor. Atmospheric movement also plays a role; certain PFAS and their precursors can volatilise during or after production and application, travelling considerable distances before settling distant from their initial sources. This air movement helps to explain the finding of PFAS in distant areas such as the Arctic and Antarctic.

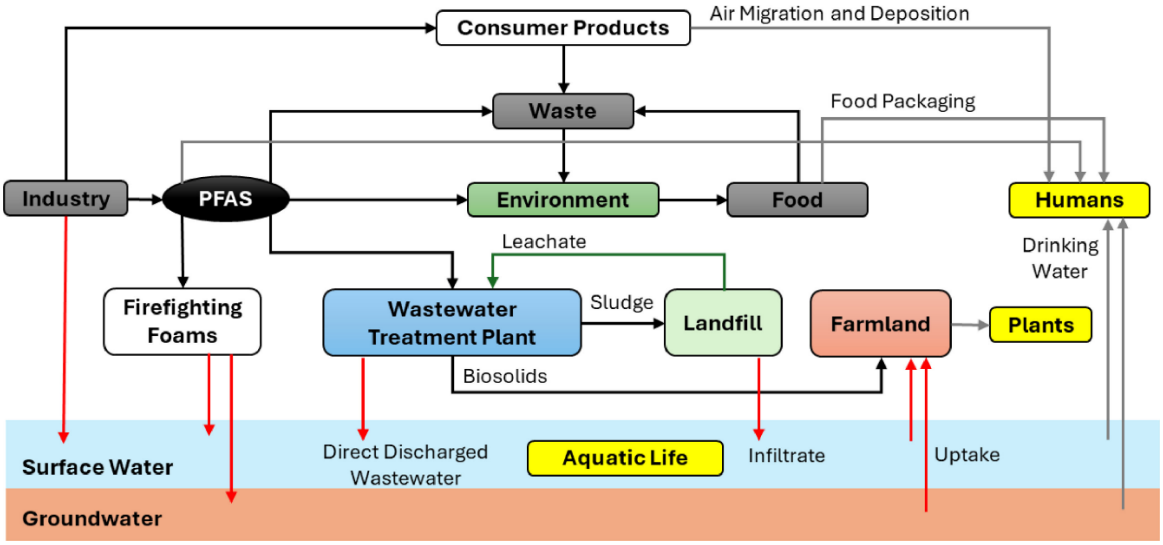

Figure 1. PFAS in the environment: sources, fate, and exposure paths. The sources of PFAS are shown in grey. Potential receptors are shown in yellow. The grey arrow illustrates probable receptor exposure paths. The red arrow indicates likely water pollution routes [23]. Reproduced with permission under the license number 6071860459239.

2.1.2. Classification of PFASs

PFAS are classified according to their structural characteristics, functional groups, and chemical properties, revealing a diverse and complex family of synthetic compounds. These compounds are linked by their unique carbon-fluorine (C-F) bonds, which contribute to their stability and resistance to degradation. Several subgroups of emerging PFASs have been identified, including short-chain PFAS (SC-PFAS), replacement PFASs, polyfluoroalkyl ether substances (PFAESs), fluorotelomer-based substances, and unregulated PFASs (Figure 2). Numerous studies have reported the classes of PFAS, including our previous study, Issaka et al. [24]. Hence, this subsection briefly discusses these various classifications.

Although most PFASs are linked by their unique (C-F) bonds, PFAESs distinguish themselves by having one or more ether linkages (-C-O-C-) in their chemical structure [25]. These ether groups can influence their physical and chemical properties, but PFAESs, like other PFASs, are also persistent in the environment. Their stability is based on fluorinated chains, and their breakdown may take diverse paths due to the ether linkages. Their widespread use and environmental durability have resulted in increased regulatory scrutiny [26,27]. Besides, SC-PFAS have a carbon backbone that is less than six atoms long for perfluoroalkyl carboxylic acids (PFCAs) and fewer than four for perfluoroalkyl sulfonic acids [28,29]. This shorter chain length allows these compounds to move more freely in the environment, has less potential for bioaccumulation, and is very resistant to removal via standard treatment techniques. Despite these characteristics, they exhibit significant environmental persistence. These compounds were frequently introduced to replace historical long-chain PFASs, but their widespread and long-term presence in ecological systems creates additional issues [28,30].

Furthermore, replacement PFASs, on the other hand, were created specifically as alternatives to longer-chain legacy substances like PFOA and PFOS [31]. Replacement PFASs, while meant to be less persistent and bioaccumulative, continue to pose hazards due to their environmental stability and unclear toxicological profiles [32]. Substances with changed chain lengths or new functional groups, for example, are designed to maintain desirable qualities such as oil and water repellence while decreasing health and environmental risks. Nonetheless, the lack of information about their destiny and toxicity causes persistent worries [31,32]. Moreover, fluorotelomer-based compounds are produced by telomerisation methods employing fluorotelomer alcohols (FTOHs) [33]. These substances usually have perfluorinated chains attached to functional end groups like acids or alcohols [33]. Fluorotelomer-based PFASs are widely used in both industrial and consumer goods due to their surfactant and repellent properties. In the environment or inside organisms, they may break down into more persistent perfluoroalkyl acids (PFAAs), adding to long-term PFAS contamination [34]. Additionally, unregulated PFASs include novel PFAS variants, precursor substances, and degradation products that fall outside of existing regulatory frameworks (Yuan et al., 2024). They exhibit a diverse range of chemical configurations and environmental behaviours and are frequently discovered using advanced analytical techniques. Despite their unregulated status, many have the same durability and potential health risks as more well-known PFASs, highlighting the critical need for research and oversight [35,36].

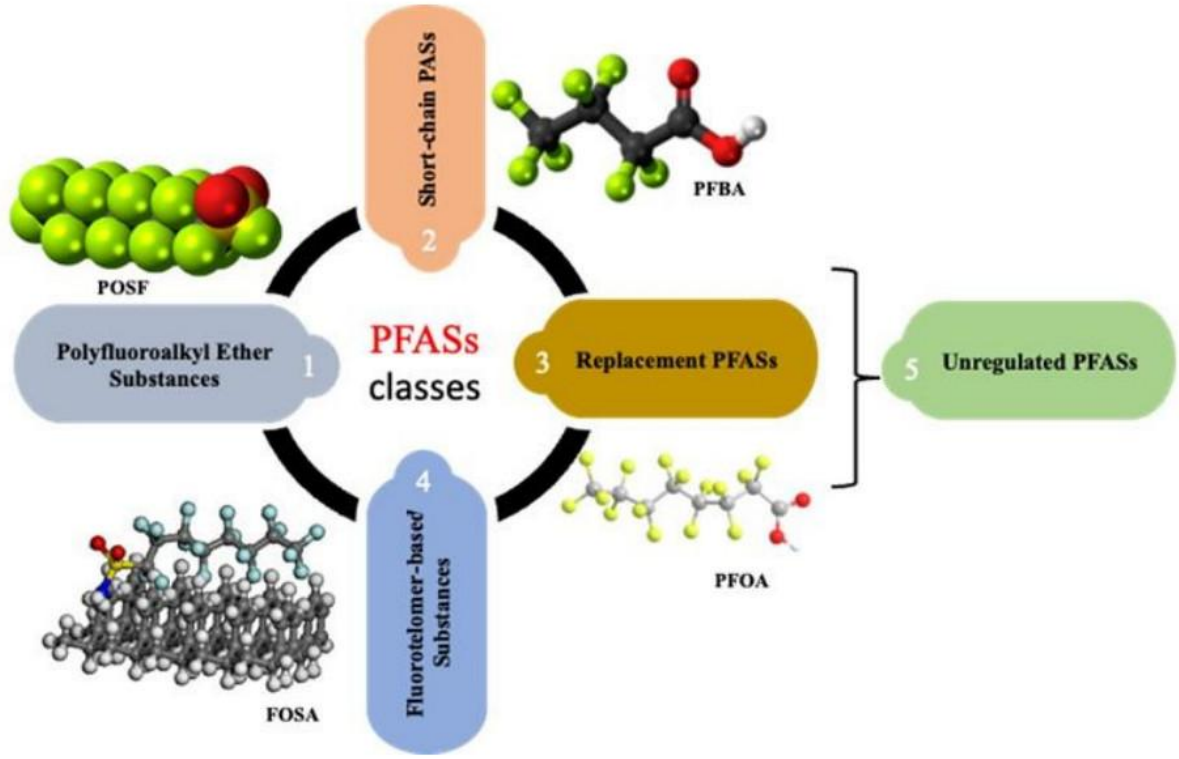

Figure 2. An illustration of SC-PFAS, replacement PFASs, polyfluoroalkyl ether substances (PFAESs), fluorotelomer-based substances, and unregulated PFASs as the main classes of PFAS [24]. Reproduced with permission under the Creative Commons Attribution (CC BY) license

2.1.3. Functional group analysis and correlation of molecular structure to adsorption potential.

PFAS's environmental behaviour and removal effectiveness are closely related to its distinctive molecular architecture, as shown in Figure 2, which consists of a hydrophobic fluorinated tail and a hydrophilic functional "head" group [37,38]. While the C-F bonds give high stability, the individual functional groups define the fundamental interaction mechanisms with carbon-based adsorbents.

PFOA and PFBA have a carboxyl group (-COOH) [39]. In aqueous conditions, they exist as negatively charged anions, rendering them sensitive to electrostatic attraction when carbon surfaces are positively charged, such as through nitrogen doping or metal impregnation [40]. This class, which includes perfluorooctane sulfonate (PFOS), has a sulfonate head group ($-SO_3^-$). Research by Leung et al. [41] suggests that PFSAs usually have greater adsorption affinities than perfluorinated compounds (PFCs) because the $-SO_3^-$ in PFSAs is larger and more electronegative than the carboxylate head group ($-COO^-$) found in PFCAs. For the same chain length, the $-SO_3^-$ group interacts more strongly with the hydrophobic aromatic domains of materials such as GAC and CNTs [42]. These molecules are distinguished by ether linkages (-C-O-C-). The presence of oxygen atoms within the chain can influence the molecular dipole and potentially facilitate hydrogen bonding with the oxygen-containing functional groups (e.g., hydroxyl and carboxyl groups) found on GO and AHC [43]. Besides, fluorotelomer-based compounds frequently contain non-fluorinated segments connected to functional groups such as alcohols. These structures can be transformed in the environment into more persistent

PFAAs, emphasising the need for adsorbents that can collect both the parent molecule and its breakdown products [44].

Furthermore, the physical properties of the PFAS molecule, particularly the perfluorocarbon chain length, are important predictors of adsorption potential [45]. Longer-chain PFAS are more hydrophobic, which serves as the principal driver for their removal via GAC, BC, and CNTs. The intensity of van der Waals forces and hydrophobic partitioning rises in proportion to the quantity of fluorinated carbons [46]. SC-PFAS, such as PFCAs with carbon backbones of less than 6 atoms, have decreased hydrophobicity and increased water mobility. Their removal is far more difficult and primarily reliant on electrostatic attraction or the fabrication of binding sites via adsorbent surface engineering [47]. The molecular configuration, whether linear or branched, also influences sorption. While linear and branched PFSA frequently exhibit similar properties, branched isomers of specific precursors have demonstrated significantly greater sorption on GAC, implying that molecular shape influences the synergy between hydrophobic and electrostatic interactions [48].

2.1.3.1. Strategies for Enhancing Short-Chain PFAS Adsorption

S-C PFAS (PFBA, PFBS) have poor hydrophobicity and rapid water mobility, resulting in early success in classic carbon-based filters such as GAC [28]. To address these restrictions, cationic surface functionalisation is one of the numerous techniques (as shown by Table 1) that have been employed. Because SC-PFAS behave less like surfactants and more like simple organic anions, electrostatic attraction must take precedence over hydrophobic contact [28]. Quaternary ammonium grafting [49] is utilised to modify carbon surfaces with high charge density quaternary ammonium groups (e.g., GTMAC), therefore dramatically increasing SC-PFAS capture by providing permanent positive sites for ionic bonding. Besides, the addition of N-based functional groups such as pyridine, benzylamine, and aniline provides opportunities for hydrogen bond formation. Studies on N-doped porous carbon beads demonstrate that these amino groups enable SC-PFAS (like PFBA) to attain better adsorption capabilities than long-chain equivalents (like PFOA) under certain circumstances [50].

Furthermore, the physical design of the carbon adsorbent is crucial in reducing internal mass transfer resistance [51]. Increasing the ratio of mesopores (2-10 nm) in the carbon structure permits SC-PFAS to circumvent competing organic matter and get faster access to interior active areas [52]. Engineering sub-nanometer holes can take advantage of "confinement effects," in which the energy required for SC-PFAS to enter the pore is reduced by the unique nanostructure, thus trapping the smaller molecules [53]. Impregnating charcoal or AC with metal nanoparticles (e.g., iron or copper-gallium co-doping) creates Lewis acid sites that can bind the anionic headgroups of SC-PFAS via complexation [54]. Finally, modified waste residues have demonstrated SC-PFAS removal efficiencies ranging from 20 % to 100 %, depending on the unique metal complexation routes produced during reduction roasting [54].

Table 1. Summary of actionable modification strategies for SC-PFAS Adsorption.

Strategies	Key Modification	Mechanism	Refs.
Cationic Surface Engineering	Grafting with cationic surfactants like CTAC or aminosilanes.	Enhances strong electrostatic attraction between the positive adsorbent surface and anionic SC-PFAS headgroups.	[55]
Metal Oxide Impregnation	Doping with Fe, Cu, or $MgAl_2O_4$ magnetic nanoparticles.	Provides Lewis acid sites and complexation pathways to bind mobile SC-PFAS. Provides Lewis acid sites and complexation pathways to bind mobile SC-PFAS.	[56]
Nitrogen Doping	Co-pyrolysis with nitrogen carriers or amination (e.g., Fe-N/BC).	Creates amine or -OH groups that promote hydrogen bonding and ionic interactions with polar head groups.	[57]
Thermal Activation	High-temperature steam activation (e.g., 900°C for AHC).	Increases microporosity and surface area to facilitate pore filling and entrapment of smaller molecules.	[58]
Structural Tailoring	Synthesis of Ordered Mesoporous Carbons (OMCs).	Optimises pore diameter (5.94–8.22 nm) to improve diffusion kinetics and minimise competition from natural organic matter.	[59]

2.1.4. Properties of PFASs

PFAS are highly hydrophobic, which means they repel water because their non-polar fluorinated carbon chains do not interact well with water molecules [60]. This hydrophobicity is complemented by their oleophobic properties, which enable PFAS to resist oils and greases. Because of these dual properties, PFAS is extremely successful at generating water- and stain-resistant coatings, which explains its extensive usage in fabrics, nonstick cookware, and food packaging [60,61]. This hydrophobic property in environmental systems, especially when paired with organic matter, improves PFAS sorption to soils and sediments, allowing them to accumulate in both terrestrial and aquatic habitats [35,62]. Beyond repellence, PFAS compounds have low surface tension, allowing them to spread uniformly across surfaces and form thin, stable films [63]. This property underlines their employment as surfactants in products such as AFFFs [64], which are widely employed in firefighting. Their capacity to adsorb to solid surfaces and soak into porous materials complicates their environmental behaviour, since PFAS can get embedded in sediment particles or soil pores via electrostatic interactions, hydrogen bonding, and van der Waals forces [42,65]. Another important characteristic of PFAS is their bioaccumulative nature [66]. These compounds resist metabolic breakdown in living organisms, resulting in accumulation in fatty tissues, particularly the liver. This bioaccumulation adds to the rising worries about human and wildlife exposure. While the toxicological profiles of PFAS vary, many have been related to liver and thyroid malfunction, immunological suppression, reproductive damage, and carcinogenesis [66,67].

2.1.5. Fate of PFAS in the environment

PFAS have some of the strongest (C-F) bonds in organic chemistry [42], making them very resistant to natural breakdown processes, including hydrolysis, photolysis, and microbial activity [68].

As a result, PFAS can remain in the environment for years or even decades without degrading. Their perseverance has given them the nickname "forever chemicals." Long-chain PFAS chemicals, such as PFOA and PFOS, are particularly persistent and pose long-term environmental concerns [69]. Besides, PFAS chemicals have great mobility, especially in aquatic environments. Most PFAS are highly water-soluble, allowing them to be easily transported through groundwater and surface water systems. Because of its mobility, PFAS discharged into the environment, whether via industrial discharge, landfill leachate, or wastewater effluent, can pollute water sources far beyond the place of release [70]. In certain circumstances, volatile PFAS precursors, such as FTOHs, can reach the atmosphere and travel considerable distances before being deposited on land or water surfaces through precipitation [71].

Another significant component of PFAS fate is its propensity for bioaccumulation. Certain PFAS, particularly long-chain chemicals, can accumulate in the tissues of living things [72]. They attach to proteins rather than lipids and tend to accumulate in the blood, liver, and kidneys. PFAS can accumulate in creatures higher up the food chain, such as fish, birds, and humans [73]. This mechanism of bioaccumulation and biomagnification raises concerns about PFAS exposure through diet, particularly in populations that rely largely on fish and game from polluted habitats [74]. Furthermore, the fate of PFAS in soil also contributes significantly to environmental pollution [75]. Some PFAS chemicals adsorb to soil particles, particularly those with longer carbon chains, whereas others are mobile and leak into groundwater [76]. The behaviour of PFAS in soil is determined by soil chemistry, pH, and organic matter concentration. In agricultural contexts, PFAS can enter the soil using contaminated biosolids, potentially altering crop uptake and entering the food chain [72,75,76].

2.1.6. Exposure pathways of PFASs

PFAS pollution of water sources is common around industrial enterprises, military bases, airports, and firefighting training grounds where AFFF have been employed [77]. These chemicals quickly permeate surface and groundwater due to their high water solubility and resistance to natural degradation. In certain areas, particularly those near polluted sites, drinking water has been discovered to have PFAS amounts significantly surpassing health recommendation standards [78]. Besides, food is another important source of PFAS exposure. PFAS may enter the food chain in a variety of ways. One approach is the pollution of agricultural soil and water [56]. When biosolids (processed sewage sludge) containing PFAS are used as fertiliser, the chemicals can be absorbed by crops or leach into irrigation water, contaminating fruits, vegetables, and cereals. Furthermore, cattle can acquire PFAS through feed and water, making meat, and milk possible sources of exposure. Moreover, PFAS are commonly discovered in fish and shellfish, particularly those taken in polluted rivers, lakes, and seas. For populations that rely largely on fishing for subsistence or cultural reasons, seafood can be a major source of PFAS exposure [56,79]. Furthermore, food packaging materials containing PFAS include grease-resistant paper, microwave popcorn packets, and fast-food wrappers. These compounds can transfer from the packaging into the food, particularly when heated, increasing exposure [80].

Additionally, inhalation is another major, but less known, route of PFAS exposure [67]. Consumer items such as stain-resistant carpets, water-repellent apparel, non-stick cookware, and coated furniture can all emit PFAS into indoor air and home dust [81]. Also, volatile PFAS precursors, such as fluorotelomer alcohols, can evaporate into indoor air and be breathed, then metabolised in the body into more persistent PFAS chemicals. Workers in sectors that make or utilise PFAS-containing chemicals are especially concerned about occupational inhalation exposure, as PFAS air concentrations

can be significantly greater than in the general environment [81]. Although cutaneous exposure is often regarded as a minor route in comparison to ingesting or inhalation, it can nonetheless occur, particularly when in contact with PFAS-treated items or polluted water. People who swim in polluted bodies of water or use PFAS-containing personal care items such as cosmetics, lotions, or sunscreens, for example, may have low skin absorption levels. However, studies show that PFAS do not readily enter the skin in considerable numbers; therefore, the health hazards from dermal exposure are often smaller than those from other routes [82].

2.1.7. Toxicological impacts of PFASs on human health

Prenatal exposure to PFAS has been linked to a variety of poor developmental effects. These include low birth weight, short gestational age, and impaired foetal growth [83,84]. Studies indicate that maternal PFAS levels, notably PFOA and 6:2 Cl-PFESA, are associated with an increased risk of preeclampsia, particularly among first-time mothers and those carrying female foetuses [85,86]. Such exposures may also raise blood pressure during pregnancy, contributing to adverse birth outcomes such as small-for-gestational-age (SGA) infants and low birth weight [87]. These early life effects demonstrate PFAS's ability to interact with the endocrine system and reproductive health by modifying hormone synthesis, disrupting metabolic pathways, and compromising foetal development [84,88]. Besides, PFAS have been shown to interfere with thyroid hormone control, potentially altering metabolism, growth, and brain function [89]. Their immunotoxic effects have also been identified, with data indicating that PFAS can suppress immunological response, change immune cell populations, and limit vaccination effectiveness. This immune suppression may raise susceptibility to infections and diminish the body's resistance to illness [61,89].

Furthermore, the liver is a primary target for PFAS buildup and damage [73]. PFAS exposure has been linked to higher liver enzyme levels, fatty liver disease, and even liver cancer. Animal studies have revealed that PFAS, such as Cl-PFESA, can cause liver enlargement, cellular vacuolation, and metabolic disturbances [73,90]. These effects are partially mediated by the activation of receptors like PPAR-γ (Singh and Chaudhary, 2025), which regulate lipid metabolism and cell differentiation. These findings imply that PFAS not only cause physical damage but also interfere with essential molecular signaling systems [73]. Also, cancer is a source of concern in PFAS toxicology [91]. Both animal and human studies have linked certain PFAS, particularly PFOA and PFOS, to an increased risk of kidney, testicular, prostate, and pancreatic cancer. Oxidative stress, immune dysregulation, epigenetic changes, and interference with receptor-mediated cellular pathways are all possible mechanisms for these carcinogenic effects [91,92]. Although PFAS are not normally genotoxic, their capacity to induce tumour growth indirectly remains a key area of continuing research [93]. Moreover, PFAS exposure influences both the cardiovascular and renal systems [94]. There have been links discovered between PFAS and hypertension, dyslipidaemia, and elevated cardiovascular disease risk. PFAS may impair kidney function and increase markers of kidney damage, possibly due to oxidative stress or tubular toxicity. Another source of worry is the neurotoxic effects of PFAS, which have been linked to altered neurotransmitter levels, poor cognitive development, and neurobehavioral disorders such as ADHD and autism spectrum disorder [41].

2.2. Traditional detection and quantification of PFASs

Owing to their ubiquitous prevalence and persistence, PFAS must be detected and quantified as

part of environmental monitoring and public health risk assessment. PFASs are notoriously resistant to environmental degradation, and even at low levels, they pose serious threats to ecosystems and human health. As a result, very sensitive and selective analytical techniques have been developed and refined for detecting and quantifying their presence in diverse media. Chromatography-based techniques for PFAS detection are among the most reliable and widely used [95], particularly LC-tandem mass spectrometry (LC-MS/MS) [96], gas chromatography-mass spectrometry (GC/ MS) [97] and high-performance liquid chromatography (HPLC) [98]. LC-MS/MS is the most extensively used method because of its high sensitivity, accuracy, and ability to analyse numerous PFAS chemicals concurrently across varied environmental and biological samples. This approach enables reliable detection even at trace levels, which is crucial considering the low concentrations at which PFAS may be harmful [95]. Besides, before analysis, PFAS must be removed efficiently from complex material matrices such as soil, water, plants, and biological tissues. Solid-phase extraction (SPE) and liquid-phase extraction (LPE) are two common sample preparation procedures used to accomplish this [99]. These strategies improve recovery while reducing matrix interferences. LPE is particularly valued for its adaptability and extraction efficiency, even though it frequently necessitates the use of significant solvents. SPE, on the other hand, is preferred due to its low solvent consumption, ease of use, and excellent reproducibility [99].

Furthermore, innovative extraction and analysis techniques have also evolved. A major accomplishment is the creation of a unique LC-MS/MS technology for analysing PFAS in plant tissues and soil, which uses optimised extraction conditions and cleaning techniques to provide high recoveries and accuracy [100,101]. In this regard, PFAS were found in various areas of Norway spruce and silver birch trees growing in polluted habitats, as reported by Nassazzi et al. [101]. Furthermore, ultra-performance liquid chromatography (UPLC) combined with Orbitrap mass spectrometry has been validated for detecting PFAS in various aquatic settings, such as seawater, lake water, and wastewater. This method demonstrated excellent linearity, sensitivity, and precision, making it suitable for measuring PFAS in real-world scenarios [102]. Additionally, rapid detection methods such as paper spray mass spectrometry (PS-MS) have gained popularity [80]. These rapid and solvent-free methods enable direct PFAS analysis in a variety of sample types, including drinking water, wastewater, and food packaging materials. PS-MS is based on the interaction of PFAS polar groups with cellulose in filter paper, which allows for selective ionisation while salts are washed away. This technique has great potential for rapid screening and field-based environmental assessments [80,103].

To address atmospheric PFAS, researchers created technologies that combine online SPE with LC-MS/MS. This method makes it easier to detect PFAS in fine airborne particulate matter at picogram levels, allowing researchers to track compounds that remain in the atmosphere and water environments long after regulatory bans have expired. These techniques are critical for monitoring both legacy PFAS and newer fluorotelomer-based alternatives. The detection and quantification of PFAS is preceded by their removal. The next section discusses the use of carbon-based materials for PFAS removal.

3. Carbon-based materials for adsorption of PFAS

Carbon-based compounds, ionic surfactants, and anion-exchange resins are the most often utilised materials for PFAS sorption in soil and water [104]. Carbon-based materials include AC, multi-walled CNTs (MWCNTs), and BC [6]. The non-polar functional groups of carbon-based materials make them excellent candidates for sorbing hydrophobic PFAS. Besides, CNTs [7] and GO [105] have demonstrated potential PFAS adsorption capabilities due to their large surface area and unique

electrical characteristics [7]. However, their use in large-scale treatment systems needs more study and evaluation of the possible health concerns connected with nanomaterials. When comparing BC, AHC, CNTs, GO and GAC (in Figure 3) as adsorbents for the removal of PFAS, each material has distinct advantages and disadvantages. Firstly, BC is more cost-effective and ecologically beneficial because it is made from biomass [106]. Surface functional groups (hydroxyl (-OH·) and carboxyl (COOH)) enhance PFAS adsorption via electrostatic and hydrophobic interactions, and they can be activated or chemically modified to suit specific purposes [106,107]. However, they have a smaller surface area and adsorption capability than sophisticated materials such as CNTs and GO [106]. Secondly, AHC has a high porosity and surface area, which is improved by chemical or thermal activation [108]. It also preserves a high degree of adjustable surface functionality and is more sustainable because it is formed from the hydrothermal carbonisation (HTC) of wet biomass. However, activation methods can raise manufacturing costs and limit environmental friendliness [109] CNTs have a large surface area and strong hydrophobic interactions, making them suitable for adsorbing non-polar PFAS [42]. They are also chemically stable and reusable and may be functionalised to improve adsorption through polar interactions with PFAS molecules [110]. However, high manufacturing costs and environmental problems associated with synthesis, large-scale application, and dispersion in water are significant hurdles [42,110]. Furthermore, GO is composed of oxygen-containing -OH· and COOH groups that interact strongly with PFAS [111]. It has high adsorption efficiency for long-chain PFAS due to hydrophobic and π-π interactions and can be used in composite materials to improve performance [112,113]. However, it is restricted by its high cost, difficult production, and possible environmental and health risks associated with GO residues [113]. GAC, on the other hand, is widely utilised, inexpensive, and commercially accessible [114]. It has high adsorption effectiveness for long-chain PFAS due to hydrophobic interactions and is easy to regenerate and reuse in a variety of applications [11]. Although it is restricted in terms of efficiency for SC-PFAS and developing pollutants, it is also sensitive to fouling from natural organic waste [11,115].

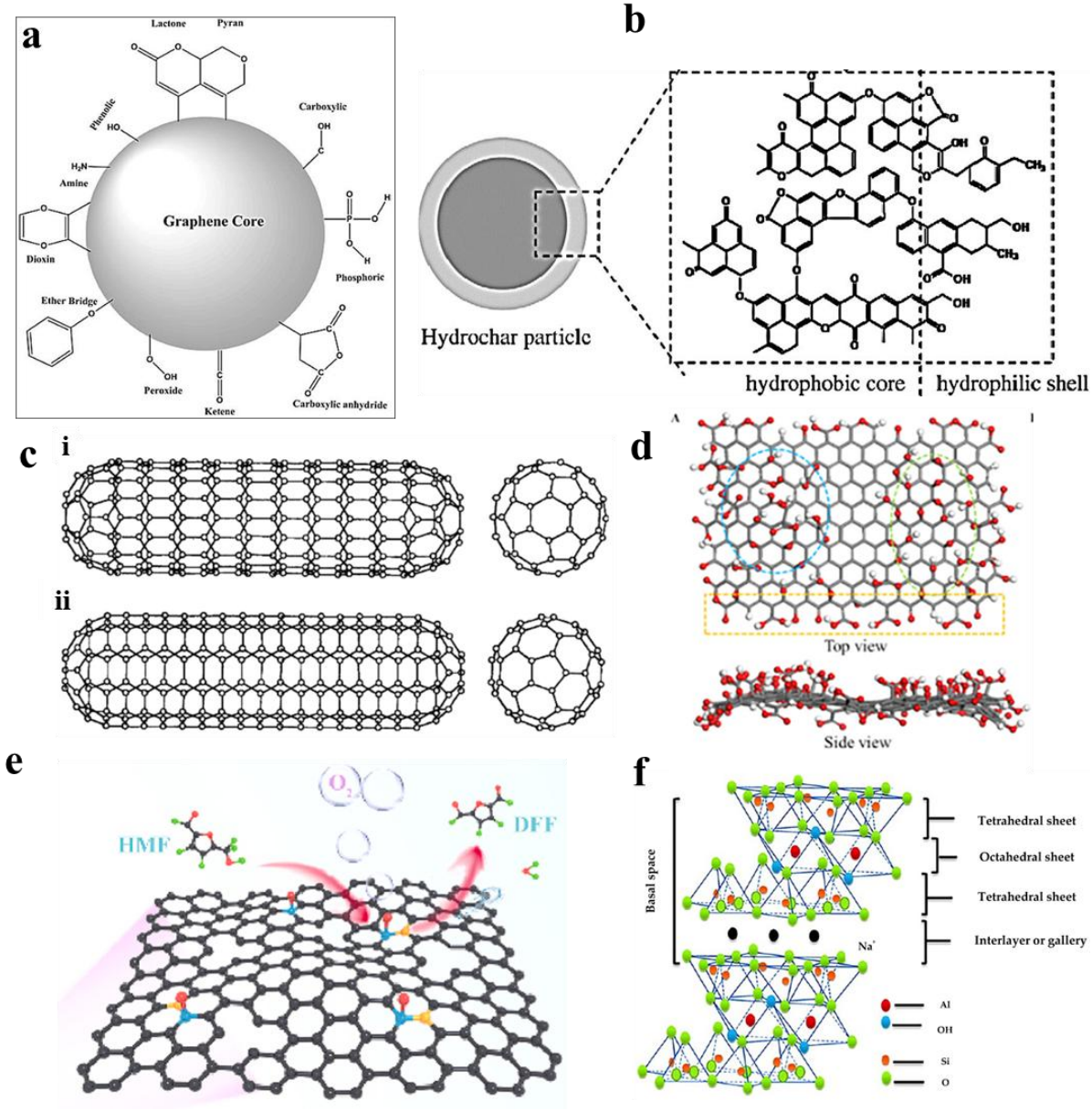

Figure 3. illustrates the structures of (a) BC with different functional groups present on its surface [116]. Reproduced with permission. Printing Press License No.: F.1 (A-4) press 2016; (b) AHC derived from cellulose with a hydrophobic core and hydrophilic shell [117]. Reproduced with permission. License number 5921900716932. (c) CNT monolayer (i) Armchair and (ii) zigzag [118]. Reproduced with permission under Creative Commons Attribution (CC BY) license; (d) GO [119]. Reproduced with permission. License number 5921910026619. (e) biomass-derived, P-doped GAC [120]. Reproduced with permission. License number 5921900716932; (f) montmorillonite [121]. Reproduced with permission under the Creative Commons Attribution (CC BY) license.

3.1. Biochar (BC) as an adsorbent

BC's large surface area, porous structure [6], and variable surface chemistry have made it a potential material for adsorbing PFASs from polluted water [15]. Owing to the environmentally

beneficial, cost-effective, and long-term alternatives of BC, it has gained tremendous attention in the environmental remediation of harmful contaminants. BC's vast surface area and microporous structure promote PFAS absorption by offering numerous interaction sites [122]. Using BC made from wood and compost, Nasrollahpour et al. [123] studied the adsorptive removal of perfluoroalkyl carboxylic acids (PFCAs), particularly perfluorononanoic acid (PFNA) and perfluorodecanoic acid (PFDA). To evaluate their effects on adsorption efficiency over time, variables like BC weight, size, and baseline PFCA concentrations were examined. At a starting concentration of 500 μg L^{-1}, the adsorption of PFDA and PFNA was 90.13 % and 85.8 %, respectively. Furthermore, altering the pyrolysis parameters (temperature, feedstock) can improve these qualities for PFAS removal [124]. BC surfaces include functional groups such as -$OH^{\cdot}$, COOH, and carbonyl groups, which allow for electrostatic and hydrophobic interactions with PFASs [125]. Chemical (such as amination and activation) and green modifications can improve adsorption efficacy even more [6]. To simultaneously remove both long-chain PFAS, primarily PFOA and perfluorooctanesulfonic acid (PFOS), from surface water matrices, Cheng et al. [126] developed an improved specialty adsorbent known as BC-based iron and perlite-integrated green environmental media (BIPGEM). When treating a combination of three SC-PFASS, including PFBA, perfluorobutane sulfonic acid (PFBS), and hexafluoropropylene oxide dimer acid (GenX Chemicals), batch-scale tests utilising BIPGEM showed that the removal efficiencies for PFOA and PFOS surpassed 98%. Besides, BC's hydrophobic areas can adsorb hydrophobic PFAS molecules, whereas π-π interactions with fluorinated PFAS structures facilitate binding. BC can be modified using additions such as metal oxides, carbon nanotubes, or surfactants to improve adsorption capacity for both long- and SC-PFAS.

3.1.1. Synthesis of biochar (BC)

A carbon-rich substance known as BC is created when biomass is thermally broken down under low oxygen levels, usually via pyrolysis, or gasification [127]. Its physical and chemical characteristics, such as surface area, porosity, and functional groups, are greatly influenced by the synthesis process and feedstock type [128]. These characteristics determine how well the material performs in applications, including energy storage, pollutant adsorption [112], and soil amendment [6].

The main process for creating BC is pyrolysis, which is the thermal breakdown of biomass at 300–700°C without oxygen [129]. In contrast to fast pyrolysis, which uses a shorter residence time at higher temperatures (400–700°C) and produces more bio-oil and syngas but less BC, slow pyrolysis uses a longer residence time at lower temperatures (300–400°C) and produces a larger output of BC [130]. The principal feedstocks are wood, organic waste, and agricultural wastes (such as maize stover and rice husks) [131]. BC with excellent stability, a wide surface area, and microporosity that is appropriate for adsorption applications is produced via pyrolysis [129,130]. Guo et al. [132] used a simple method of direct pyrolysis from lignin waste at a low temperature to create nitrogen and iron co-doped BC (Fe-N/BC). By adding electrophilic groups, Fe and N may significantly increase the BC surface's electron transfer capacity in addition to promoting physical characteristics, including compact pores, high surface area, stable crystal, and magnetic recyclable ability. Furthermore, using a slow pyrolysis technique, Handiso et al. [133] examined how pyrolysis temperatures affected the physicochemical characteristics of BC produced from pine wood. Analysis using Fourier transform infrared (FTIR) spectroscopy revealed that the BC produced at various temperatures had unique functional groups. According to the elemental analysis, the concentration of carbon (C) increased as the pyrolysis temperature increased, whereas the concentrations of oxygen (O) and hydrogen (H)

decreased in proportion.

Gasification is the process of converting biomass at temperatures exceeding 700 °C with little oxygen into charcoal, syngas, and ash [134]. Because of the increased processing temperature, the BC has more porosity and fewer volatile materials [134,135]. To maximise syngas production and produce BC in a fixed-bed horizontal tube furnace reactor, Abioye et al. [86] investigated the co-gasification of sugarcane bagasse (SB) and palm oil decanter cake (PODC). Using the Box-Behnken design and Response Surface Methodology, operating factors such as temperature (700-900 °C), biomass ratio (30–70 wt%), and particle size (0.25–2 mm) were optimised. The BC was subjected to analyses; under ideal circumstances, 900 °C, 42 wt% PODC biomass ratio, and 2 mm particle size produced a syngas volume of 41.5 vol% and a BC of 0.3 wt%. BC with a mesoporous structure was identified by Brunauer-Emmett-Teller (BET) analysis. Its surface area was 398.55 $m^2 g^{-1}$, its pore diameter was 6.49 nm, and its pore volume was 0.13 $cm^3 g^{-1}$.

3.2. Hydrochar (HC) as adsorbent

The process of HTC includes the thermal breakdown of wet biomass in water at low temperatures (180–250°C) and high pressures (usually 2–10 MPa), ideal for wet feedstocks that do not need to be dried, including food waste and sewage sludge [136]. This creates HC with more functional groups that include oxygen for better adsorption [137]. Wang et al. [138] used Co-HTC of waste medium-density fiberboard (MDF) and different nitrogen carriers to create N-containing chemicals (NCCs) and N-enriched HCs. The effects of the MDF: N carrier mass ratio and the kind of N carrier (melamine, urea, or chitosan) on yield and production distribution were examined. The electrochemical performance of N-rich HC as a precursor for supercapacitor materials was investigated, and the creation process and potential reaction pathways of NCCs in bio-oil and N-doped BC were clarified. Besides, Tan et al. [139] investigated the effects of a modified reaction medium on the HTC-linked pyrolysis process by converting rice straw (RS) in two stages. RS was first hydrothermally treated in a modified reaction medium (metal chlorides and ammonium persulfate, AP) and a conventional medium (water). The resulting HC was then upgraded by pyrolysis. The properties of the HC and the modified pyrolysed HC were investigated. A modified reaction medium was demonstrated to increase the bulk yield of HC. Modified HC had a lower carbon and oxygen content and a greater ash and fixed carbon content than standard HC.

3.2.1. Activated hydrochar (AHC) as an adsorbent material

Produced by HTC, AHC is a modified type of HC that goes through extra activation procedures to improve its adsorption capabilities [140]. Because of its characteristics, it shows promise as an adsorbent for eliminating PFASs from water [109]. The creation of functionalised materials with increased surface areas, porosities [10], and surface chemistries essential for PFAS remediation are made possible by the combination of hydrothermal processing and activation procedures [141]. AHC has shown promise for adsorbing perfluoroalkyl sulfonic acids (PFSA), PFCAs, and emerging PFAS. The findings showed that AHC has a comparatively large specific surface area [142]. Notably, the AHC outperformed previously reported sorbents in terms of sorption partition coefficient values, demonstrating positive sorption performance for all tested PFAS. AHC made from waste and renewable biomass is consistent with the ideas of the circular economy. Hydrochar's activation improves performance and may even be able to compete with activated carbon, a popular adsorbent.

Additionally, activation and modification enable customisation for certain PFAS adsorption issues, such as branched and SC-PFAS.

3.2.2. Synthesis of activated hydrochar (AHC)

AHC is primarily produced through HTC's synthesis. Biomass feedstocks, such as agricultural wastes and lignocellulosic materials, are processed in water at moderate pressures (2–10 MPa) and temperatures (180–250°C) [143]. HC, a carbonaceous solid containing oxygenated functional groups, is produced throughout the process. Physical techniques are used to activate the HC that is created. HC is treated with gases such as CO_2 or steam to improve porosity and surface area at temperatures between 700 and 900°C [144]. Chemical activation improves the interaction with PFAS molecules by increasing microporosity and functionalisation by the application of activating agents such as potassium hydroxide (KOH), phosphoric acid (H_3PO_4), or Zinc chloride ($ZnCl_2$). Khoshbouy et al. [145] used HTC to create sludge-based AHC (SAHC) from wastewater sludge with a high moisture content (88.9 %) without pre-drying, followed by chemical and physical activation using KOH and CO_2, respectively. Additionally, via final analysis, the impacts of activation techniques and HTC temperatures (170, 200, 230, and 260 °C) on the physicochemical properties of HC and SAHCs were examined. The findings showed that, even at 900 °C (261.6 m^2 g^{-1}), KOH-activation at 700 °C could considerably increase the surface area of AHC (from 6.3 to 1613.9 m^2 g^{-1}) in comparison to CO_2-activation. Furthermore, Zubbri et al. [146] employed a lignocellulosic precursor, a rambutan peel (RP), to create AHC by pre-treating the biomass with water and then hydrothermally carbonising it. The produced hydochar was then activated using KOH under a range of operating parameters, such as varying activation temperatures (600–900 °C), activation durations (60–180 min), and KOH: AHC ratios (1:1–4:1), to improve the microporosity. When activated with a 2:1 KOH: AHC ratio at 850 °C for 120 minutes and a water-soaking pre-treatment, the KOH-activated AHC had the maximum CO_2 adsorption capability.

Additionally, the addition of functional groups (like amine or -OH·) promotes electrostatic interactions with PFASs [147], and the addition of metal impregnation (like iron or aluminium) enhances the adsorption of PFAS types through complexation or ion exchange [144,145]. A collection of novel organically functionalised layered double hydroxide (LDH) adsorbents for the removal of PFAS, with a major focus on PFOA, Min et al. [148] developed, characterised, and evaluated. Through a post-grafting procedure, the organic functional groups were covalently bonded to the Zn-Al LDH. Because of the synergy between the modified organic functional groups that provide enhanced hydrophobic interactions to capture PFOA and the positively charged structural layers of LDHs that provide strong electrostatic interactions, the organically functionalised LDHs were very effective for PFOA adsorption.

3.3. Carbon nanotube (CNTs) as an adsorbent material

Owing to its huge specific surface area, which usually ranges from 100 to 1000 m^2 g^{-1}, CNTs offer PFAS molecules plenty of active sites to be adsorbed [149]. Unusual Structure: CNTs are made of a network of interconnecting pores that are hollow and cylindrical. PFAS adsorption is made easier by this special structure on both the interior and exterior surfaces. CNT surfaces may be chemically altered to add different functional groups, which will increase their PFAS affinity and boost adsorption efficiency [150]. Strong adsorption can result from CNTs interacting with PFAS molecules via a

variety of processes, including hydrophobic interactions, π-π interactions, and electrostatic forces. Song et al. [151] used the layer-by-layer assembly technique to create MWCNTs on magnetic carbon (Fe_3O_4@C) nanospheres, which were then used to extract six PFAS from environmental water samples using ultra-high-performance liquid chromatography (HPLC) coupled with tandem MS. The as-prepared MWCNTs@Fe_3O_4@C were characterised. The key extraction parameters were carefully tuned using the Box-Behnken design. Under ideal conditions, good outcomes were obtained. The synthesised sorbent has a wide linear range (0.1–1000 ng L^{-1}), low detection limits (0.03–0.09 ng L^{-1}), and high repeatability (3.80 9.52 %) in extracting and detecting six PFAS.

3.3.1. Synthesis of carbon nanotubes (CNTs)

CNTs are generated utilising a variety of processes to tailor their dimensions [152], structures and characteristics to specific uses [153]. Chemical vapour deposition (CVD) [154]. Arc discharge (AD) and laser ablation are the three most used ways of producing CNTs [155]. CVD generates solid deposits by reacting gases or steam in the gas phase or at a gas-solid interface [155,156]. This process includes gas diffusion on the substrate surface, gas adsorption on the substrate surface, and chemical reactions on the substrate surface to form solid deposits and gas-phase byproducts that are separated from the substrate surface [156]. In an inert gas environment, an electric furnace is utilised to heat the furnace, after which carbon-containing gases are continually fed over the catalyst. The catalyst fractures the material to give carbon atom clusters, which are progressively deposited on the solid support housing the catalyst, generating CNTs on the surface of the catalyst or substrate [156].

AD approaches are potential ways for creating high-quality CNTs [157]. The AD process involves evaporating graphite anodes at high temperatures to generate very crystalline CNTs with a nearly flawless graphite lattice structure [158]. The atmospheric pressure and catalyst are crucial factors influencing the quality of CNTs in AD methods. According to Zhou et al. [157], high-purity graphite powder served as the carbon source, while iron (Fe) acted as the catalyst to manufacture defect-free MWCNTs using direct-current AD in a nitrogen environment. Different pressures and catalysts were tested to see how they affected CNT yield and shape. As the nitrogen pressure within the vacuum chamber rises, the MWCNTs grow longer and more upright. Fe has a high defect repair efficiency, allowing for the synthesis of MWCNTs with flawless lattices and no defects. It was discovered that MWCNTs are mostly located in the Fe mesh near the cathode. The results demonstrated that the approach was less expensive, more repeatable, and produced high-quality, defect-free MWCNTs than the standard AD method. Furthermore, Madhurima et al. [159] used the AD approach to synthesise CNTs, with a major focus on improving process parameters such as gas pressure and arcing voltage. The study also investigated the practical applications of these CNTs, testing their ability to adsorb Methyl Orange (MO) and Rhodamine B (RhB) dyes. The results showed that CNTs performed moderately, with 16 % removal efficiency for MO and 60 % for RhB dyes under identical experimental circumstances. Carbon soot, on the other hand, displayed extraordinary performance, with removal efficiencies of 53 % for MO and an astonishing 82 % for RhB dyes, owing to their large specific surface area.

A high-powered laser ablates a graphite target containing a metal catalyst (Ni or Co) in an inert gas environment to produce CNTs [160]. As the vapour cools, the carbon condenses into CNTs. This approach yields high-purity CNTs with fewer flaws and is suitable for laboratory-scale single-walled carbon nanotube (SWCNT) production [161,162]. Ismail et al. [163] demonstrated how to generate MWCNTs and carbon nanoparticles (C NPs) utilising pulsed laser ablation of a graphite target in water

without the need for a catalyst. The influence of laser wavelength on optical absorption and structural attributes was investigated, and the synthesised CNTs were found to be polycrystalline, with a peak associated with the diamond structure. The investigation revealed that the average diameter of CNTs synthesised with 532 nm was 20 nm and a few micrometres in length, but CNTs synthesised with 1064 nm had an average diameter of 75 nm and lengths of a few sub-micrometres. Besides, Chrzanowska et al. [164] investigated the influence of laser wavelength on the yield and characteristics of SWCNT. CNTs were produced using a double-pulsed Nd: YAG laser with wavelengths of 355 or 1064 nm. The transmission-synthesised CNTs were examined using scanning electron microscopy/scanning transmission electron microscopy (SEM/STEM) microscopy and Raman spectroscopy. The results demonstrated that the practical range of UV laser radiation fluence is shorter, and that the characteristics of synthesised CNTs are considerably more sensitive to laser fluence than those under infrared laser radiation.

3.4. Graphene oxide (GO) as an adsorbent material

With a high specific surface area (usually 500–2600 $m^2 g^{-1}$), GO provides PFAS molecules with an abundance of adsorption sites [65]. GO comprises a layer of carbon atoms organised in a hexagonal lattice, each atom thick. For PFAS molecules, this two-dimensional shape offers a high density of adsorption sites. GO has a variety of oxygen-containing functional groups, including COOH, epoxy, and -OH, which can interact electrostatically, via hydrogen bonding, and π-π interactions with PFAS molecules. The ability of GO sheets to stack and create stable dispersions in water helps PFAS adsorption at the water-GO interface [165]. A new kind of GO-based adsorbent was described by Pervez et al. [166], which also evaluated how well it removed PFAS from water. With an almost 100 % removal rate for all 11 PFAS tested, GO-cetyltrimethylammonium chloride (CTAC)-GO (GO-CTAC-GO) modified by the cationic surfactant CTAC was determined to be the best of the eight adsorbents tested. The suggested adsorption processes, including hydrophobic and electrostatic interactions, were validated by thorough characterisation [166]. In addition, according to Tunioli et al. [167], β-cyclodextrin (βCD) modified GO nanosheets with varying-sized alkyl linkers (GO-Cn-βCD) were synthesised and used as PFAS sorbents in drinking water. By functionalising βCD with an amino group that was still awaiting, the resultant precursors were grafted onto GO nanosheets using an epoxide ring-opening process. Adsorption experiments on PFBA, a very persistent PFAS used for the case study, demonstrated that the alkyl linker length had a significant impact on the effectiveness of adsorption [167]. Although GO shows promise for the PFAS adsorption of metal ions [168], PFASs [169] from water environments, there are worries about their possible negative effects on the environment [170] and health, like oxidative stress, DNA damage, inflammatory response, apoptosis [171], autophagy and necrosis [172]. More study is required to assess its long-term efficacy, safety, and economic viability in real-world PFAS cleanup applications.

3.4.1. Synthesis of graphene oxide (GO)

GO is a functionalised derivative of graphene that is rich in oxygen-containing groups (such as -OH, COOH, and epoxide groups) [173], making it hydrophilic and chemically adaptable [9,173]. GO is typically synthesised by oxidising graphite using a variety of techniques [168]. Hummer's approach has received a lot of interest in the manufacture of GO since it is both efficient and frequently used for scalable synthesis. However, it produces toxic waste and necessitates cautious handling due to the

exothermic nature of the reaction and poor yield. Zhang et al. [174] devised an improved Hummers technique for synthesising GO that uses boric acid (H_3BO_3) instead of sodium nitrate ($NaNO_3$). This change reduced the reaction time to 1 hour at room temperature, successfully suppressed the synthesis of carbonyl and COOH, eliminated the emission of hazardous gases nitrogen dioxide (NO_2) and dinitrogen tetroxide (N_2O_4), and increased GO yield by 10 %. While the shape of GO synthesised using the modified Hummers approach, as detected by SEM and transmission electron microscopy (TEM), was comparable to that of the classic Hummers method, Raman analysis revealed that the GO produced herein had fewer structural flaws. Also, Marcano et al. [175] discovered that removing $NaNO_3$, increasing the quantity of Potassium permanganate ($KMnO_4$), and executing the reaction in a 9:1 combination of sulphuric acid/phosphoric acid (H_2SO_4/H_3PO_4) improved oxidation efficiency. This enhanced process produces more hydrophilic oxidised graphene material than the Hummers' method or the Hummers' method with added $KMnO_4$. Furthermore, even though this approach produces more oxidised GO than Hummers' method when both are reduced in the same chamber with hydrazine, chemically converted graphene (CCG) created by this novel method has equal electrical conductivity. Unlike Hummer's process, the new technology produces no hazardous gas and can be readily regulated.

3.5. Granular activated carbon (GAC) as an adsorbent material

GAC generally has a surface area of 500–1500 $m^2\ g^{-1}$, which is rather large [176]. The adsorption capability is increased by this huge surface area, which offers PFAS molecules several adsorption sites. The porous structure of GAC is well-developed and has a wide variety of pore sizes, including macropores (>50 nm), mesopores (2–50 nm), and micropores (<2 nm) [177]. GAC can absorb PFAS molecules of different shapes and sizes thanks to its hierarchical pore network. Functional groups, including COOH, -$OH^{\cdot}$, and phenolic groups, are present on the surface of GAC and can interact with PFAS molecules by a variety of processes, such as hydrogen bonding, hydrophobic interactions, and electrostatic attraction. With the ability to remove both long- and SC-PFAS from water, GAC has a high adsorption capacity for PFAS because of its wide surface area, porous structure, and surface chemistry [177]. PFAS molecules are rapidly adsorbed from water by GAC; the adsorption equilibrium is frequently attained in a matter of minutes to hours. For useful applications in water treatment, this quick adsorption is advantageous. Furthermore, GAC can be regenerated to regain its adsorption capability by employing chemical, biological, or thermal methods. As a result, GAC is used for a variety of purposes, cutting waste and improving the treatment process's economics [177,178].

Powdered or granulated AC proved effective in removing PFOA and PFOS from soil and water [149]. A small number of commercial adsorbents on the market might be employed in conjunction with or instead of AC. GAC is the most widely utilised adsorbent for PFAS removal [179]. It has a large specific surface area, a microporous structure, and a variety of pore diameters, allowing it to adsorb both long and SC-PFAS. GAC can be utilised in fixed-bed filters or as a powdered material in batch treatment systems [30]. Sadia et al. [179] examined the sorption of PFAS on GAC (Figure 4). The study used ecologically relevant PFAS concentrations and a realistic water-to-GAC ratio, giving realism that is typically neglected in previous investigations. Three distinct types of GACs were tested, with varied micropore and mesopore structures. The sorption studies employed tap water spiked with 5 ng/L of each of 31 PFAS, including linear and branched isomers, as well as three sets of PFAS precursors. There were no significant variations in PFAS sorption among the three GACs investigated. Except for the SC-PFAS PFAS precursors, the majority of the PFAS analysed had a clearance rate of less than 50 %. For PFAS, both carbon chain length and functional groups influenced sorption, but for

PFAS precursors, neither did. The addition of ether linkages and sulfonamide groups significantly improved sorption. Linear and branched PFSA had equal sorption properties; however, branched isomers of sulfonamide acetic acid precursors had considerably greater sorption. This suggests that sorption was influenced by both hydrophobic and electrostatic interactions [179].

Notwithstanding these benefits, PFAS content, water quality, and the existence of competing pollutants can all have an impact on how well GAC performs. It is crucial to take these into account and modify operating parameters, such as contact duration, adsorbent dose, and pretreatment needs, to maximise GAC's efficacy in PFAS cleanup.

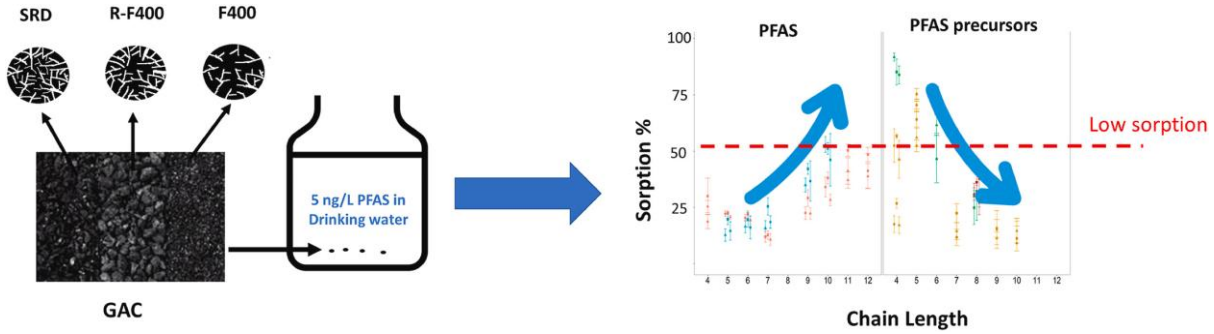

Figure 4. Schematic illustration of the sorption of PFAS and its precursors on activated carbon under realistic drinking water conditions [160]. Reproduced with permission under Creative Commons CC-BY license.

3.5.1. Synthesis of granular activated carbon (GAC)

GAC is preferably generated from hard biomass materials such as coconut shells and palm kernels. To obtain GAC, these shells are activated physically and/or chemically [180]. The proposal of Liang et al. [181] was to create a reactive GAC coated with pyrite (FeS_2) for environmental remediation that would integrate the functionalities of GAC adsorption and FeS_2 reduction. GAC-FeS_2 composite materials were effectively made using successive methods (incipient wetting iron impregnation, transformation into hematite (Fe_2O_3) by calcination at 300 °C, and sulfurisation by calcination at 400 °C). The point of zero charge (pHPZC) of GAC washed with nitric acid (HNO_3) was reduced to facilitate the drawing of iron ionic species into the pores of GAC, and FTIR data supported the dominance of carboxylic acid groups, resulting in a negatively charged GAC surface. The XRD findings showed that the calcined composites are transitional GAC-Fe_2O_3 and final GAC-FeS_2. Furthermore, a simple and environmentally favourable approach for the synthesis of granular fuel and GAC was established. The findings revealed that at the ideal temperature of 230 °C, the high heat value, energy density, and equilibrium moisture content of granular fuel were 23.53 MJ kg^{-1}, 35.87 GJ m^{-3}, and 0.73 %, respectively. GAC had great compression strength, which made it suitable for use in an adsorption bed. The ideal temperature for granular fuel and GAC characteristics was determined to be 230 °C, with GAC having a BET surface area of 641 m^2 g^{-1} and an iodine adsorption value of 626 mg g^{-1}. As environmental issues gain prominence, granular fuel and GAC may be viable and eco-friendly materials for future uses.

4. Mechanisms of adsorption and adsorption models

The adsorption of PFAS onto carbon-based materials is driven by a series of physicochemical interactions that may be quantified using known adsorption models. Understanding these processes is critical for improving material design and forecasting performance in practical applications.

PFAS molecules have hydrophobic fluorinated chains that preferentially interact with the hydrophobic surfaces of GAC and other materials. This hydrophobic partitioning is a main driver for the adsorption of long-chain PFAS; the strength of interaction increases with chain length. Hence, hydrophobic Interactions are one of the most predominant adsorption mechanisms for the removal of PFAS by carbon-based materials [182]. Besides, electrostatic attraction is particularly important for PFAS containing charged functional groups (such as $-COO^-$ and sulfonates) [183]. The strength of these interactions is influenced by the adsorbent's surface charge and the pH of the solution. For example, basic and hydrophobic activated carbon surfaces promote PFAS adsorption, but increasing surface acidity can limit absorption [183,184]. Furthermore, some carbon-based adsorbents, particularly those with functionalised surfaces, can remove PFAS using anion or ligand exchange processes [110]. This is especially critical for SC-PFAS, where ionic interactions are more important. The adsorbent's pore size distribution and nanostructure are crucial to its adsorption effectiveness. Water trapped in nanopores, as well as the presence of air nanobubbles within activated carbon cavities, can help to remove SC-PFAS. Mesoporous carbons with customised functionalities (e.g., fluorination) can enhance adsorption capacity and selectivity [110]. Also, modification of carbon surfaces (e.g., amination, fluorination, or defunctionalisation) might boost adsorption by enhancing hydrophobicity or creating binding sites, thereby strengthening the interaction with PFAS molecules [185].

4.1. Adsorption models

Adsorption models are critical for characterising and forecasting the behaviour of PFAS absorption on carbon-based adsorbents [185]. These models aid in the interpretation of experimental data, adsorbent performance comparisons, and treatment system optimisation. In addition, adsorption models explain the connection between the quantity of PFAS adsorbed onto the adsorbent and its equilibrium concentration in solution at a given temperature [183]. Understanding these isotherms is critical for assessing adsorbent efficacy, improving treatment procedures, and creating prediction models for environmental cleanup.

4.1.1. Langmuir isotherm model

The Langmuir isotherm is a fundamental concept in surface chemistry that describes how molecules adsorb to solid surfaces [186]. It is especially useful for studying the adsorption of pollutants such as PFAS onto carbon-based materials. The Langmuir isotherm assumes that adsorption occurs through a dynamic equilibrium between molecules in the fluid phase (gas or liquid) and those bonded to a solid surface. The model depicts a solid surface with a finite number of identical adsorption sites, each capable of storing a single adsorbate molecule. Adsorption and desorption are reversible processes, and equilibrium occurs when their rates are equal [187,188]. Furthermore, the Langmuir model is based on several assumptions, such as all adsorption sites are identical and energetically equivalent, each site can hold only one molecule, once occupied, no further adsorption can occur at that site (no multilayer adsorption), adsorbed molecules do not interact with each other, the adsorption of one

molecule does not affect the adsorption of another, adsorption and desorption processes are reversible and reach equilibrium, and the system is isothermal [188].

The Langmuir isotherm model may predict the adsorption of PFAS onto the surface of carbon-based adsorbent materials. It relates the amount of adsorbate adsorbed per unit mass of adsorbent (q_e) to the equilibrium concentration of the adsorbate in the fluid phase (C_e) [189]. The Equation can be written as:

$$q_e = \frac{k_L C_e q_{max}}{k_L + C_e + 1} \quad (1)$$

Where q_e = equilibrium adsorption capacity (mg g^{-1}), q_{max} = maximum adsorption capacity (mg g^{-1}), C_e = PFAS concentration at equilibrium (mg L^{-1}), and K_L = Langmuir constant based on pollutant adsorption sites (L mg^{-1}).

4.1.2. The Freundlich isotherm model

The Freundlich isotherm model is an empirical equation that is commonly used to describe adsorption processes on heterogeneous surfaces [190]. Unlike the Langmuir model, which assumes monolayer adsorption on a homogeneous surface, the Freundlich isotherm takes into consideration the variety of adsorption sites and energies seen on real-world adsorbents such as activated carbon, BC, and other porous materials [190,191]. The Freundlich model posits that the adsorbent surface is heterogeneous, containing spots with different adsorption energies. It does not limit adsorption to monolayers; multilayer adsorption is feasible, particularly at higher concentrations. The heat of adsorption reduces logarithmically as coverage rises, indicating the variety of binding sites. The model is not developed from basic theory, but matches a wide variety of experimental data, particularly for adsorption from solutions and at low to moderate concentrations [190,192].
The Freundlich isotherm is mathematically expressed as:

$$q_e = K_f C_e^{1/n} \quad (2)$$

Where q_e = K_f = Freundlich constant associated with the adsorption capacity (mg/g) (L mg^{-1}), (1/n) = the adsorption intensity of the adsorbent.

4.2. Adsorption kinetics models

Adsorption kinetics describe the reaction rate and sorption process, which includes mass transfer, diffusion, and reaction on the adsorbent surface during adsorption [193]. Adsorption of adsorbates from water-soluble mixtures onto the adsorbent involves external mass transfer over the boundary layer or diffusion film between the liquid phase and the adsorbent's outer surface; diffusion within the adsorbent particles, allowing the adsorbate solution to enter the adsorbent pores; and the formation of physicochemical interactions of the adsorbate at the active centres in the pores [194,195]. Pseudo-first-order and pseudo-second-order models are commonly used kinetic models for monitoring the kinetics of adsorption processes, whereas interfacial and particle diffusion models are commonly used to identify the mechanism of sorption [194].

4.2.1. The pseudo-first-order kinetic model

The pseudo-first-order kinetic model, also known as the Lagergren model, is a popular method for modelling the kinetics of adsorption processes, particularly those dominated by physical adsorption on homogeneous surfaces. It reveals how rapidly an adsorbate (such as PFAS, dyes, or metals) is absorbed by an adsorbent (such as activated carbon or charcoal) over time [196]. The model assumes that all adsorption sites on the adsorbent are energetically equal and that no interactions occur between adsorbed molecules [197]. It is particularly useful when the adsorption process is dominated by weak van der Waals forces rather than chemical bonds. Adsorbate molecules often diffuse through the boundary layer around the adsorbent particles, rather than intraparticle diffusion or surface reaction, which is the rate-limiting step. The model highlights the significance of exterior (film) diffusion in regulating the total adsorption rate [196,197].

The Equation can be written as:

$$\ln(q_e - q_t) = \ln q_e - k_1 t \quad (3)$$

Where qq_t = amount of pollutants adsorbed at time t (mg/g), k_1 = first-order rate constant (min^{-1}).

4.2.2. The pseudo-second-order kinetic model

The pseudo-second-order kinetic model is one of the most extensively used models for characterising adsorption kinetics, especially in systems with chemisorption, where the adsorption rate is regulated by chemical interactions between the adsorbate and the adsorbent surface [198]. The model implies that chemisorption is the rate-limiting phase, which involves valence forces via electron sharing or exchange between the adsorbent and adsorbate [199]. It supports adsorption on heterogeneous surfaces, with adsorption capacity proportional to the square of the number of empty sites. The pseudo-second-order kinetic model applies to a wide range of adsorbate-adsorbent systems, including PFAS, heavy metals, dyes, and pharmaceuticals, and is frequently found to be a better match than the pseudo-first-order model in many real adsorption processes [199,200].

The differential equation for the pseudo-second-order kinetics is given by:

$$\frac{t}{q_t} = \frac{1}{k_2 q_e^2} + \frac{t}{q_e} \quad (4)$$

Where k_2 = second-order rate constant (g mg^{-1}).

4.3. Synergistic interactions between carbon-based materials and PFAS

Carbon-based materials and PFAS interact synergistically, which aids in the adsorption 870 and removal of these persistent pollutants from water. These interactions are controlled by the physicochemical properties of both PFAS molecules and carbon-based adsorbents, such as surface chemistry [168], porosity [117], hydrophobicity [201], and electronic properties. Besides, the synergy is based on the high affinity between the fluorinated carbon chains of PFAS and the hydrophobic surfaces of GAC, powdered AC, CNTs, GO, and BC [202]. The non-polar, hydrophobic tails of PFAS molecules align with the non-polar, aromatic domains on the surface of carbon adsorbents, resulting in van der Waals forces and π-π interactions [38]. These forces promote the initial attraction and

retention of PFAS molecules on the adsorbent surface. The longer the PFAS carbon chain, the stronger the interactions, which explains why long-chain PFAS like PFOA and PFOS are more easily adsorbed on activated carbon than their short-chain counterparts [38,203]. Additionally, electrostatic interactions play a key role in the adsorption process, particularly when carbon compounds are functionalised to increase surface charge [204]. PFAS molecules are typically found in water as negatively charged anions due to their $-SO_3^-$ or $-COO^-$ groups. Carbon surfaces modified to have positive charges, such as those doped with nitrogen, metals, or quaternary ammonium groups, can bind PFAS anions more efficiently via ionic interactions. This electrostatic attraction complements hydrophobic bonding, resulting in a synergistic process that improves total PFAS uptake [204].

Furthermore, the presence of oxygen-containing functional groups on carbon-based materials, such as hydroxyls, carboxyls, or carbonyls, may also aid in hydrogen bonding with the polar head groups of PFAS [205]. Though weaker than hydrophobic or electrostatic forces, these interactions can still improve PFAS adhesion, particularly when dealing with shorter-chain compounds with lower hydrophobicity [206]. Besides, porosity and surface area enhance synergistic interactions [165]. Highly porous materials, such as AC and certain engineered BC, have numerous surface sites and pore structures that can trap PFAS molecules. The synergy here comes from the combination of high surface accessibility and favourable surface chemistry, which results in both quick adsorption kinetics and high capacity [205]. Finally, graphene-based materials and CNTs exhibit a more advanced form of synergy due to their tunable surface properties and high aspect ratios [207]. These nanostructures enable precise functionalisation, improving both hydrophobic and electrostatic interactions concurrently [205,207]. Fluorinated or amine-functionalised graphene oxide, for example, has greater PFAS selectivity due to higher binding affinities, demonstrating a cooperative interaction between the material's surface structure and the PFAS molecular architecture [208].

5. Application of carbon-based materials for the removal of per- and poly-fluoroalkyl substances (PFAS)

To treat PFAS contamination, many strategies have been developed; they may be generally divided into two categories: in situ and ex-situ procedures. The ex-situ methods include adsorption, where GAC [178], ion exchange resins, GO [209] have demonstrated promising results for PFAS removal from water [24]; membrane filtration, where reverse osmosis (RO), nanofiltration (NF) [210], and ultrafiltration (UF) [211] can effectively remove PFAS from water, with UF being more effective for long-chain PFAS and RO and NF being more effective for SC-PFAS [212]; advanced oxidation processes (AOPs) [213], where ozonation, UV irradiation, and photocatalysis can produce reactive oxygen species (ROS) that can degrade PFAS [214,215]; and chemical oxidation, where advanced oxidation techniques like electrochemical oxidation [216] and sulphite-based oxidation systems have demonstrated potential for treating PFAS-contaminated water. To lessen the mobility and bioavailability of PFAS in contaminated water and soils, in situ procedures such as soil cleaning, thermal desorption, and in situ stabilisation can be used [217]. Installing permeable reactive barriers (PRBs) with adsorbent materials like BC, AHC, GO, GAC and CNT can intercept and treat PFAS-contaminated groundwater plumes. For the removal of PFAS, Table 2 summarises the numerous methods that rely on adsorption for PFAS remediation. Ease of use and environmental friendliness present carbon-based materials as innovative adsorbents for removing PFASs from a variety of environments.

Table 2. Summary of the various adsorbent materials for PFAS remediation.

Method	Absorbent framework	Type of PFAS	Adsorption kinetics	Isotherm models	Adsorption capacity	Refs
Carbon-based NMs for PFAS adsorption						
Adsorption on CNTs (mWCNT)	Multi-walled carbon nanotube-filled electrospun nanofibrous membranes (MWCNT-ENFMs)	PFOS	The pseudo-first-order and pseudo-second-order models	Freundlich model, Langmuir model and partition–adsorption model	16.29±0.26 μmol g^{-1}	[218]
	Multi-wall carbon nanotubes (MWCNTs)		Dubinin-Ashtakhov	Freundlich model	np	[219]
	MWCNTs					[219]
	MWCNTs					[220]
	MWCNTs					[221]
	MWCNTs		The pseudo-first-order and pseudo-second-order models	Freundlich model	Removal efficiency: 20 to 30 %	[222]
Adsorption on CNTs (sWCNT)	Single-wall carbon nanotubes (SWCNT)		Pseudo-second-order model	Langmuir and the Freundlich models	170 mg g^{-1}	[223]
Metal-organic frameworks (MOFs) for PFAS adsorption						
Adsorption on novel metal-organic framework (MOF)	Modified Al-based MOF (MIL-96) with hydrolysed polyacrylamide with surface amine groups (MIL-96-RHPAM2)	PFOA	Pseudo-second-order model	Freundlich models	340 mg g^{-1} (72 hours)	[224]
Adsorption on RMSDN600	Red mud-modified sawdust (RMSDN600)	PFOS	The pseudo-first-order and pseudo-second-order models	Langmuir and the Freundlich models	194.6 mg g^{-1}	[225]
Adsorption on Zirconium-based metal-organic framework (MOF)	Zirconium-based metal-organic framework (MOF)	PFSAs, PFCAs	The pseudo-first-order and pseudo-second-order models	Langmuir and the Freundlich models	PFSAs = 400 to 620 mg g^{-1} PFCAs = 201 to 604 mg g^{-1}	[226]
Adsorption on Cu/F-rGA	Cu nanoparticles and fluorine-modified graphene aerogel (Cu/F-rGA)	PFOS	The pseudo-first-order and pseudo-second-order models	Langmuir, Freundlich, and model 3	0.5–10 mg L^{-1}	[105]

Adsorption on CAMTAg	Activated maize tassel silver (PAMTAg) and chemically activated maize tassel silver (CAMTAg)	PFOS PFOA	The pseudo-first-order and pseudo-second-order models	Langmuir and the Freundlich models	PFOS = 454.1 mg g^{-1} PFOA= 321.2 mg g^{-1}	[12]
Adsorption on AE-APTMS	N-(2-aminoethyl) amino propyltrimethoxysilane (AE-APTMS)	PFOA, PFOS	Pseudo-second-order model	Langmuir and the Freundlich models	Removal efficiency: PFOS= 78 % PFOA= 65 %	[227]
Adsorption on Fe_3O_4@GAC, Fe_3O_4 NPs	Granular activated carbon-supported magnetite nanoparticles Fe_3O_4@GAC, Fe_3O_4 NPs)	PFOA	Pseudo-second-order model	Langmuir and the Freundlich models	Removal efficiency: 28.8 %	[228]
Granular activated carbon (GAC) for PFAS remediation						
Adsorption on GAC	Minicolumn tests	PFOA and PFOS	The pseudo-second-order model	np	Removal efficiency: 20 % (PFOA) and 55 % (PFOS)	[229]
Adsorption on GAC	np	PFOA and PFOS	The pseudo-second-order model	np	Removal efficiency: 73 %–97 %	[230]
Adsorption on colloidal activated carbon (CAC)	np	PFAA, PFOA and PFOS	np	Langmuir and the Freundlich models	np	[231]
Adsorption on the clay content	np	PFOA and PFOA	np	Langmuir and the Freundlich models	Removal efficiency: 75 %	[232]
Adsorption on GO	Cetyltrimethylammonium chloride (CTAC)-GO	PFAS	The pseudo-second-order model	Langmuir, Freundlich, Sips, and Toth models	Removal efficiency: 100 %	[233]

Notes: np= not provided.

5.1. Granular activated carbon (GAC) for PFASs remediation

Table 3 provides a summary of comparative analysis: the performance, chemistry, and physical forms of GAC versus clay and MOFs. GAC is utilised as the model carbon-based material since it is the most often used and thoroughly researched kind of carbon-based material in water treatment and environmental remediation applications. It also has numerous major advantages, including high surface area and porosity, versatility in physical forms, proven performance, and a comparable standard [234,235]. Owing to these advantages, Yuan et al. [229] extracted GAC from six filter-adsorbers used in three drinking water treatment plants in Ontario, Canada, for taste and odour control. They next assessed the GAC's ability to remove PFOA and PFOS using minicolumn experiments

conducted under various operating circumstances. It was shown that even after a lengthy duration of GAC operation, the GAC could remove between 20 % and 55 % of PFOA and PFOS. Also, the PFAS removal performance of GAC and ion exchange resin (IX) was assessed and compared utilising a segmented column system with full-scale media operating under continuous flow conditions (Figure 5). The results of the PFAS breakthrough study performed using column operation at various empty bed contact times (EBCTs) were utilised to characterise the mass transfer zone (MTZ) of numerous PFASs and determine the best EBCTs for GAC and IX treatment [236].

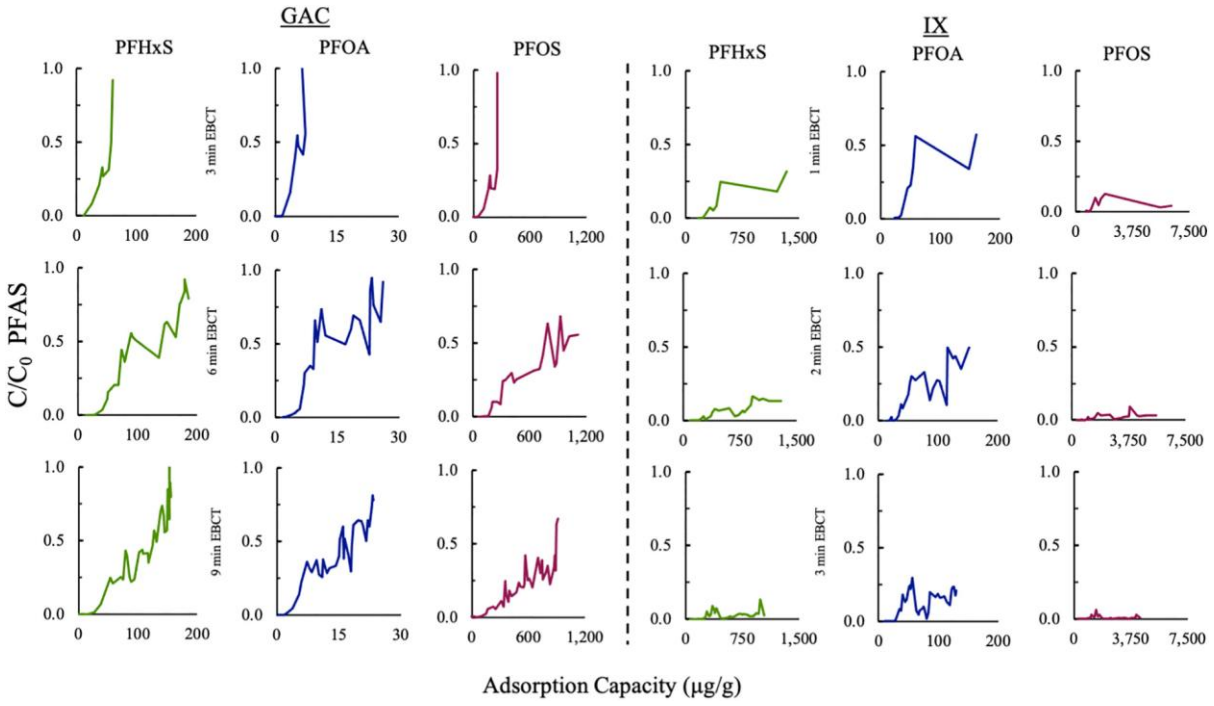

Figure 5. Schematic illustration of PFAS treatment with GAC and ion exchange resin: Comparing chain length, empty bed contact time, and cost [236]. Reproduced with permission. License number 5850010329790.

Besides, smouldering combustion was investigated by Duchesne et al. [237] as a remediation method for PFAS-impacted GAC and PFAS-contaminated soil. GAC was used as the additional fuel to promote smouldering in combinations containing sand, PFAS-spiked laboratory-constructed soil, and PFAS-impacted field soil. Both fresh and PFAS-loaded GAC were used. Using soil and emission tests, including targeted PFAS and suspect screening in addition to hydrogen fluoride and total fluorine, the fate of PFAS and fluorine was assessed. The findings showed that smouldering occurred spontaneously at temperatures over 900 °C when the GAC content of the soil exceeded 35 g/kg. The treated soil's post-treatment PFAS contents were either close to or below the detection limits (0.0004 mg/kg). Furthermore, compared to 16 % of the PFAS on soil, 44 % of the original PFAS on GAC underwent complete elimination. In the quantified analytical suite, PFAS accounted for less than 1 % of the original PFAS contamination on GAC or soil. The remaining ones, according to the results, were likely volatile fluorinated chemicals and modified, shorter-chain PFAS that were successfully cleaned with GAC. Total organic fluorine analysis worked well for GAC loaded with PFAS in the sand; however, non-PFAS interfered with soil analysis [237]. Besides, using GAC and anion exchange

column tests, McCleaf et al. [238] examined the effects of perfluorocarbon chain length, functional group, and isomer structure on the removal of various PFASs. Over 217 days, the elimination of 14 distinct PFASs was observed. Because dissolved organic carbon (DOC) and PFASs are abundant in the absorbents, the results demonstrate the selective nature of PFAS removal. The length of the perfluorocarbon chain and the effectiveness of PFAS removal using GAC and AE were shown to be positively correlated, and PFASs with $-SO_3^-$ functional groups were more effective at being removed than those with carboxylate groups. In a similar vein, the time-to-column breakthrough increased as the length of the perfluorocarbon chain rose and was longer for the PFSAs for both GAC and AE than for the PFCAs. As the experiment concluded, longer-chained PFASs showed greater removal, suggesting agglomeration or micelle formation, while shorter-chained PFASs demonstrated desorption behaviour [238].

Furthermore, GAC may be regenerated to restore its adsorption capability via thermal, chemical, or biological techniques. Proper disposal or regeneration of wasted GAC is critical for preventing the release of adsorbed PFAS into the environment. GAC-based PFAS remediation has several obstacles, including limited adsorption capacity, high costs for large-scale applications, and the requirement for regular GAC replacement or regeneration. Research is being conducted to produce more efficient and sustainable GAC-based PFAS treatment methods.

Table 3. Summary of comparative analysis: the performance, chemistry, and physical forms of carbon materials versus clay and MOFs.

Comparative analysis: the performance						
Adsorbents	Typical Adsorption Capacity	Selectivity	Regeneration	Cost	Application Range	Refs
Carbon-based material: GAC	High (up to 980 mg/g for dyes; high for PFAS and organics)	Moderate; improved by surface modification	Moderate; thermal/chemical methods	High (relative to clays)	Water/air purification, ESD, EMI shielding	[234,235]
Clays	Moderate (6–289 mg/g for dyes; improved with modification)	Can be tailored by activation/composites	Good; low energy required	Very low (0.04–0.12 USD/kg)	Water treatment, CO_2 capture, barrier creams	[239,240]
MOFs	Very high (often surpassing AC and clays for emerging contaminants)	High, tunable by linker/metal choice	Varies; some are unstable in water	High (lab scale)	Gas separation, water purification, and advanced catalysis	[241,242]
Comparative analysis: chemistry						
Adsorbents		Key Functional Groups/Features		Mechanisms		Refs
Carbon-based material: GAC		Aromatic rings, oxygen-containing groups, tunable by activation		Hydrophobic, π–π, electrostatic, pore-filling		[234,235]

Clays	Silicate layers, exchangeable cations, modifiable with organics or metals	Ion exchange, hydrogen bonding, surface complexation	[239,240]
MOFs	Metal centres, organic linkers, customisable pores	Coordination bonding, size exclusion, functional group interactions	[242,243]

Comparative analysis: physical Forms

Material	Powder	Beads	Films	Monoliths	Composites	Refs
Carbon-based material: GAC	Yes	Pellets and beads	Coatings	Yes	MOFs, clays, polymers	[243]
Clays	Yes	Granules, beads and composites	Films and creams	Yes	BC-clay and polymer-clay	[239]
MOFs	Yes	Embedded in beads/polymers	Thin films	Yes	MOF-carbon, MOF-clay	[243]

5.2. Graphene oxide (GO) for PFASs remediation

Owing to its special qualities, including its large surface area, adjustable surface chemistry, and superior mechanical and thermal stability, GO has become a potential material for PFAS remediation [244]. GO can interact with PFAS molecules by a variety of processes, including electrostatic contacts, hydrogen bonding, and hydrophobic interactions. It also possesses a wide surface area and an abundance of oxygen-containing functional groups [209]. Moreover, GO can be supplemented with other functional groups or NPs to increase its ability to remove PFAS. Adding MOFs [245], functionalising with nanomaterials like CNTs or metal NPs (Me NPs), and grafting with cationic polymers or molecules are examples of common alterations. Concerning PFAS remediation, these changes increase GO's selectivity and adsorption effectiveness. To intercept and handle PFAS-contaminated groundwater plumes, GO can be incorporated into PRBs. GO is a desirable material for passive and long-term PFAS cleanup due to its strong reactivity, stability, and ease of functionalisation [246]. The total cost of PFAS treatment can be decreased by using GO-based adsorbents, which can be repeatedly manufactured and utilised. Solvent washing, thermal treatment, and electrochemical regeneration are examples of regeneration techniques [247].

A new kind of GO-based adsorbent was described by Pervez et al. [233], who also evaluated how well it removed PFAS from water (Figure 6). With an almost 100% removal rate for all 11 PFAS tested, GO-CTAC-GO modified by the cationic surfactant cetyltrimethylammonium chloride (CTAC) was determined to be the best of the eight adsorbents tested. The pseudo-second-order model provided the best description of the adsorption kinetics, indicating fast adsorption. The suggested adsorption mechanisms, including electrostatic and hydrophobic interactions, were confirmed by detailed characterisation using SEM-energy dispersive X-ray spectroscopy (SEM-EDX), FTIR, thermogravimetric analysis (TGA), X-ray diffraction (XRD), and X-ray photoelectron spectroscopy (XPS). Remarkably, neither the pH of the solution nor the ionic strength nor the presence of natural organic matter affected the performance of GO-CTAC [233]. Besides, Bresnahan et al. [248]

concentrated on deriving design principles using functionalised graphene materials from molecular dynamics simulations of PFAS. The interactions between PFBA, PFOA, PFOS and graphene, GO functionalised with nitrogen groups, partially fluorinated flakes, and graphene were investigated using simulations. To investigate how interactions between flakes could result in competitive interactions about PFAS or pore development, five flakes were employed in each simulation. The results of the investigation showed that PFAS adsorption is influenced by both the flake's functional groups and clustering mechanisms. The following functionalisations are the most effective for PFAS adsorption: amine and amide-functionalised GO flake, completely fluorinated GO, and pure graphene. The materials were more likely to adsorb long-chain PFAS and -SO_3^- PFAS than SC-PFAS and carboxylic head groups.

GO is regarded as an environmentally benign substance, and its use in PFAS remediation is consistent with sustainable development and green chemistry concepts. But it's important to carefully consider any potential environmental effects of GO-based materials, particularly considering GO's movement and fate in aquatic ecosystems. Research on GO remediation for per- and polyfluoroalkyl substances (PFAS) is now underway to optimise GO alterations, characteristics, and treatment methods to maximise PFAS removal efficiency. These compounds can be useful in tackling environmental PFAS pollution as more potent GO-based cleanup techniques are created.

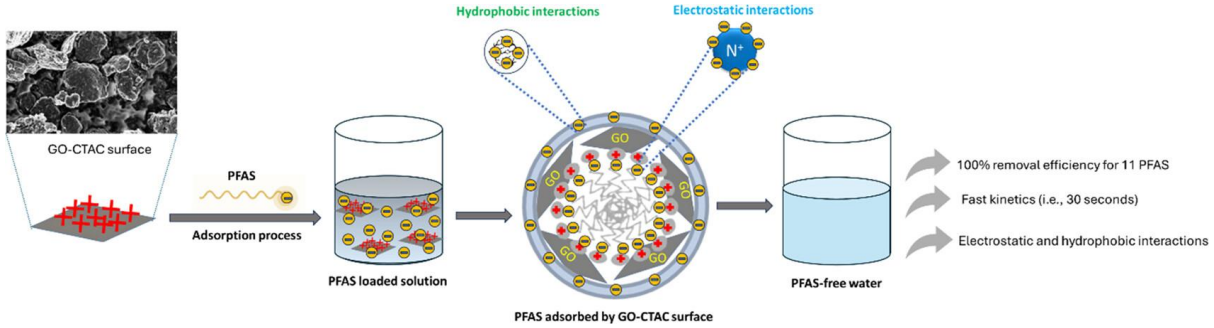

Figure 6. Schematic illustration of the surface modification of GO for fast removal of PFAS mixtures from River Water [233]. Reproduced with permission under CC-4.0 license.

5.3. Carbon nanotube (CNTs) for PFASs remediation

Because they differ from standard adsorption technology and have unique features [249], nanomaterials (NMs) can overcome many of the problems associated with their corresponding bulk materials [250]. One of the main disadvantages of using NPs is their high cost when compared to other adsorbents and their equivalent bulk materials [251]. Nonetheless, they are thought to be incredibly effective and efficient materials for removing a variety of contaminants [252]. Carbon-based NMs, particularly CNTs, MWCNTs and SWCNTs [253], have a high adsorption capacity, a large specific surface area, strong hydrophobicity, and stability under most environmental conditions [7]. Therefore, with some degree of success, CNTs have been used extensively as adsorbents to remove contaminants from wastewater, including PFAS [7,253]. CNTs have some benefits over NMs and other carbon-based materials. CNTs often attain adsorption equilibrium more quickly than conventional carbon-based materials [254]. For PFAS adsorption, for instance, chars, GAC, resins, and ash take longer than two days to achieve equilibrium, while CNTs do so in just one day [255]. Similar to CNTs, other carbon-based nanomaterials (NMs) can be employed as general adsorbents in water treatment applications.

These include fullerenes, graphene, GO, reduced GO (rGO), and carbon nanospheres [253,255]. While graphene, GO, and rGO have recently been employed in the manufacture of carbon-based aerogels for PFAS removal [7], there are few reports of their usage in the nanoscale domain [254].

Most researchers agree that the primary interaction for PFAS adsorption on CNTs is hydrophobicity [11,227]. The degree of hydrophobicity of the PFAS alkyl chain has been demonstrated to be closely correlated with PFAS adsorption on CNTs [220]. The adsorption of PFAS on CNTs may be negatively impacted by electrostatic interactions. Because PFAS in water are frequently anionic and CNTs' exposed surfaces are typically negatively charged, unfavourable electrostatic interactions result [256]. Nonetheless, the widespread consensus is that the attractive hydrophobicity of the CNT surface outweighs these opposing repulsive electrostatic interactions [257]. H-bond-induced secondary interactions appear to have little impact on PFAS adsorption processes as well [256]. Since CNTs usually have few or no exposed hydrogen atoms on their surface, PFAS fluorine atoms cannot form an H-bond with them. Even though MWCNTs have a higher number of exposed hydrogen atoms, studies [223,256] indicate that these interactions are still minimal when compared to hydrophobic effects. Lastly, colligative van der Waals forces are minimal and π–π interactions are not possible since PFAS do not include π systems. Figure 7 indicates that the PFAS and CNT adsorption process includes H-bond-induced secondary contacts, electrostatic interactions, and hydrophobicity.

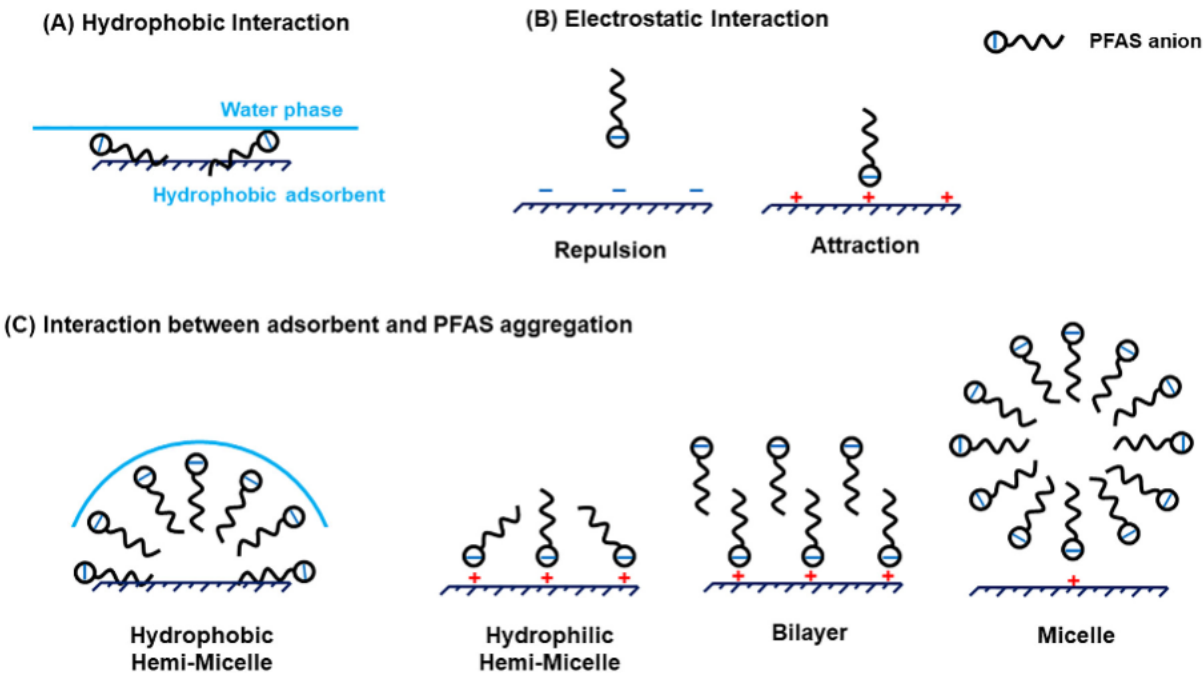

Figure 7. Illustration of the PFAS and CNT adsorption process, including H-bond-induced secondary contacts, electrostatic interactions, and hydrophobicity [256]. Reproduced with permission. License number 5756961143298.

Besides, a new family of effective adsorbents known as ordered mesoporous carbons (OMCs) has highly ordered pores with an average diameter ranging from 5.94 to 8.22 nm [258]. Their pore volumes vary from 1 $cm^3\ g^{-1}$ to 1.54 $cm^3\ g^{-1}$, and their specific areas span from 1276 to 1396 $m^2\ g^{-1}$ specific surface area [258]. OMCs have been used extensively for the adsorption of organic contaminants from water because of their benefits. After being created by Lei et al. [258], OMCs with various oxygen

concentrations were initially employed to adsorb PFOA from aqueous solutions. The oxygen-rich OMC-700 has a lower PFOA adsorption capability than the lower oxygen-content OMC-900. When compared to other adsorbents reported in the literature, OMCs achieve the adsorption equilibrium faster. A significant factor in the quick adsorption kinetics is the mesopores. The kinetic data were more closely matched by the pseudo-second-order model. The Freundlich isotherm model provides a good match for the experimental results, so the multilayer adsorption approach was suggested for PFOA adsorption onto OMCs. During the adsorption process, micelle or hemi-micelle structures may develop. Because of the divalent bridge and salting-out effects, PFOA adsorption was positively impacted by a variety of background salts. Humic acid competes with OMCs for adsorption sites, which might result in a noticeable decrease in PFOA adsorption. The adsorption findings supported the predicted hydrophobic interaction and electrostatic interaction adsorption processes. The OMC is a promising adsorbent for the elimination of PFOA in engineering applications due to its high adsorption capacity and quick adsorption kinetics [258].

New strategies, including integrated techniques that absorb and eliminate PFAS and high-capacity, selective sorbents with quick absorption and regeneration, are made possible by NM technology. The kinetics and selectivity of PFAS physical removal and destruction can be improved by nano-enhanced materials, and the treatment materials may be recyclable or reusable. Additionally, there are chances to enhance the effectiveness of most traditional remedies with nanoscale technology. This section discusses several new nano-enhanced methods for treating PFAS in aqueous media.

5.4. Activated hydrochar for PFASs remediation

AHC, which is produced from biomass by hydrothermal carbonisation (HTC) [259], shows promise in eliminating PFAS from water, providing a sustainable and possibly cost-effective option. It has a wide range of real-world applications, including the treatment of polluted groundwater, wastewater, and soil. The efficiency of AHC originates from its large surface area and adjustable characteristics, which enable it to absorb PFAS from water [145]. AHC successfully removes PFAS through large surface area and adjustable surface chemistry, attaining ≥80 % removal of long-chain PFAS (PFOS, PFOA) and ≥70 % removal of SC-PFAS (PFBA) when steam activated at 900°C [260]. Besides, AHC has enhanced sorption capacity by hydrophobic interactions, electrostatic forces, and pore constriction, comparable to GAC but with cheaper production costs [142]. Chen et al. [142] prepared AHC for sorbing ten PFAS, including five PFCA, three PFSA, and GenX chemicals (Figure 8). The results showed that AHC has a reasonably large specific surface area (207 m^2/g) and hydrophobic surface characteristics. The AHC demonstrated good sorption ability for all evaluated PFAS, with log K_d values that exceeded those of other reported sorbents (0.83 for GenX on pyrochar and 2.83 for PFOA on commercial BC). Furthermore, AHC can also catalyse the breakdown of PFAS under alkaline hydrothermal conditions (for example, >99% PFOS degradation) [261].

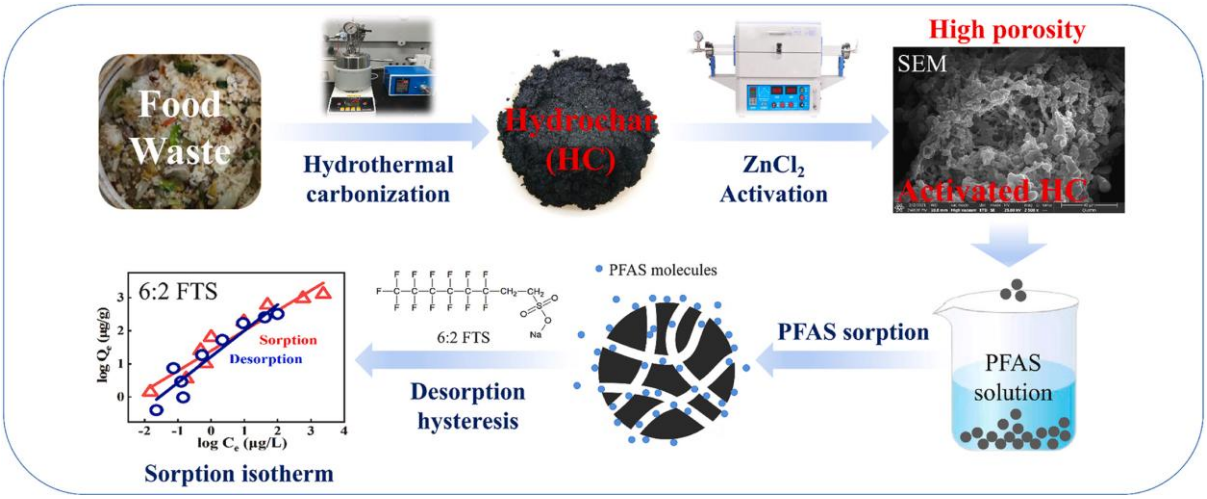

Figure 8. Illustration of food waste prepared AHC for sorbing ten PFAS, including five PFCA, three PFSA, and GenX chemicals [142]. Reproduced with permission. License number 6055301080833.

5.5. Biochar (BC) for PFASs remediation

Pristine BC, made by pyrolysing agricultural or forestry waste, has a porous structure and surface chemistry that can adsorb PFAS via hydrophobic interactions and electrostatic attractions. However, unmodified BC's effectiveness is typically moderate, with removal rates SC-PFAS (such as PFBA and PFBS) ranging from 56 % to 63 % and somewhat higher for long-chain PFAS, depending on feedstock and pyrolysis conditions [262]. Recent research has focused on improving BC performance by activation and surface modification [6]. Functionalised BCs, such as those impregnated with nanoparticles (e.g., iron), metal oxides, or surfactants, exhibit dramatically increased PFAS adsorption, with removal efficiencies equivalent to or greater than that of some commercial activated carbons. MgO and $MgFe_2O_4$ magnetic nanoparticles (MNPs) were combined with BC using a co-precipitation and slow pyrolysis technique to remove hazardous PFOA and PFOS from synthetic aqueous solutions (Figure 9) by Naz et al. [263]. The nanocomposites demonstrated high selectivity against PFOA/PFOS, maintaining an efficiency of over 80 % over five cycles. The hypothesised mechanism of PFOA/PFOS with $MgFe_2O_4$-BC demonstrated that electrostatic and hydrophobic interactions are the primary driving forces for sorption. Besides, BC-based composites, such as BIPGEM, have been shown to remove over 98 % of long-chain PFAS in batch experiments and over 85 % in fixed-bed column investigations, demonstrating their promise for real-world water treatment applications. Increasing the pyrolysis temperature over 400 °C enhances the hydrophobicity, surface area, and pore structure of BC, further boosting PFAS absorption [264,265].

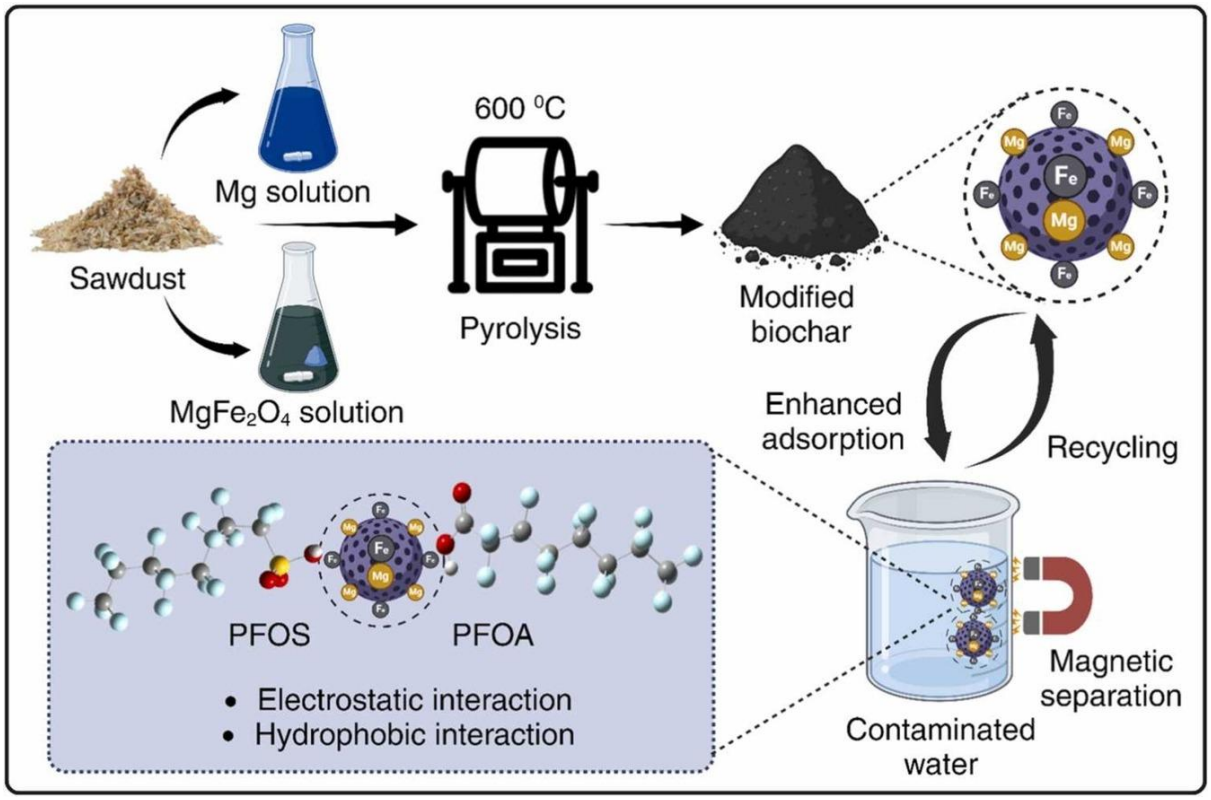

Figure 9. Illustration of efficient removal of PFOA and PFOS from aqueous solution using MgO and $MgFe_2O_4$ modified BC [263]. Reproduced with permission. License number 6055350908438.

5.6. Comparison of carbon-based materials for adsorption

The choice of a carbon-based adsorbent for PFAS removal is a complicated interplay of efficiency, cost, and environmental impact [68]. While GAC is still the industry standard because of its commercial availability and proven performance, newer nanomaterials such as CNTs and GO provide improved kinetics and capacity [256]. In contrast, sustainable alternatives like BC and AHC [145] are gaining favour for their circular economy benefits [128]. To intuitively illustrate the trade-offs between these materials, Table 4 compares their typical performance, chemistry, and physical forms. Furthermore, the moisture level of the available biomass feedstock frequently influences the decision between BC and AHC, with HTC (for AHC) being optimal for wet wastes such as sewage sludge or food waste.

Table 4. Comparative analysis of carbon-based adsorbents for PFAS removal.

Adsorbent	Key Advantages	Main Limitations	Adsorption Mechanisms	Relative Cost	Refs.
GAC	Commercially mature; high capacity for long-chain PFAS.	Poor performance for SC-PFAS PFAS; sensitive to NOM fouling.	Hydrophobic partitioning, pore-filling.	Moderate	[266,267]
BC	Very low cost; carbon-negative; derived from waste biomass	Lower surface area; moderate efficiency for short-chain species.	Electrostatic attraction, hydrophobic interactions	Low	[264,268]
AHC	Sustainable synthesis from wet waste; highly tunable surface chemistry	Variable quality based on feedstock; higher activation energy costs.	Hydrophobic interactions, electrostatic forces	Low-medium	[128,144]
CNTs	Extremely fast kinetics; high surface area; chemically stable	High production cost; potential for aggregation and toxicity.	π–π interactions, hydrophobic bonding.	High	[7,118,152]
GO	Exceptional density of functional sites; stable in water dispersions	High cost; difficult large-scale recovery; health risks.	Hydrogen bonding, electrostatic, π–π.	Very high	[9]

5.7. Practical cases and methods for regeneration and reuse

Sustainable management of PFAS-containing adsorbents is critical for avoiding secondary environmental contamination and lowering operational expenses. While GAC is the most recognised material for full-scale regeneration, newer carbon compounds like GO and AHC are being explored for new recovery strategies [269]. Besides, thermal treatment is the most often used commercial approach for GAC regeneration (as shown in Table 5). Thermally reactivated GAC was compared to virgin GAC in large-scale water treatment plants like Cincinnati to determine changes in pore structure and performance [178]. Smouldering combustion has been tested as an on-site remediation option for PFAS-contaminated GAC. This method uses the GAC as a fuel source to achieve temperatures above 900°C, resulting in the total removal of 44% of the original PFAS on the GAC, with the remaining transformed to shorter-chain volatile fluorinated compounds [270]. Furthermore, chemical technologies allow for on-site regeneration without the considerable energy consumption of thermal furnaces. This new method has been shown to successfully desorb PFAS from used GAC under mild circumstances, allowing for numerous reuse cycles without degrading the adsorbent's physical

qualities [271]. For GO and CNTs, solvent washing and electrochemical regeneration are emerging as efficient ways to repair adsorption sites [272]. AHC is a unique substance that may act as both a sorbent and a catalyst. AHC has been demonstrated to accelerate the breakdown of PFOS in alkaline hydrothermal conditions, with degradation rates exceeding 99 %. This integrated technique enables simultaneous removal and destruction, which improves the treatment train's sustainability [273].

Table 5. Summary of Regeneration Techniques for Carbon-Based Adsorbents

Method	Targeted Material	Key Mechanism	Performance Outcome	Refs.
Thermal Reactivation	GAC	High-temperature volatilisation	Restores pore structure; proven at full-scale	[178]
Smoldering Combustion	GAC	Self-sustaining oxidation (>900°C)	44% total PFAS elimination from GAC	[271]
Supercritical CO_2	GAC	Pressure-induced desorption	Maintains adsorbent properties over cycles	[271]
Alkaline Hydrothermal	AHC	Catalytic degradation	>99% PFOS destruction	[274]
Solvent Washing	GO / CNTs	Solubilisation of PFAS	Laboratory-scale site recovery	[275]

5.8. Challenges associated with carbon-based adsorbents for PFAS removal

The utilisation of GAC, AHC, BC, GO, and CNT shows great potential, although each strategy has limits and areas for development. Understanding these material-specific challenges and limitations is essential for advancing their practical application for PFAS removal.

GAC is the most proven carbon-based adsorbent for PFAS removal, particularly for PFOA and PFOS. GAC's performance is dramatically reduced for short-chain and branched PFAS, which are less hydrophobic and interact less strongly with the carbon surface [142,276]. When treating water with a high concentration of these chemicals, a breakthrough occurs sooner, and the service life is shortened. The presence of natural organic matter (NOM) reduces GAC effectiveness by occupying adsorption sites and deactivating surfaces [276]. While some GAC formulations (such as those with a greater surface area or positive charge) can enhance removal rates, the underlying issue of SC-PFAS attraction remains. Additionally, regeneration of wasted GAC is energy-intensive and may not completely restore adsorption capability.

GO has a high theoretical adsorption capacity due to its huge surface area and abundance of oxygen-containing functional groups that can interact with PFAS through hydrogen bonding and electrostatic attraction [277]. However, GO is expensive to make in large quantities, and its inclination to agglomerate in water can diminish effective surface area and adsorption effectiveness [278]. The present practical usage of GO is limited by its environmental destiny, possible toxicity, and recovery and regeneration issues.

CNTs have strong hydrophobic and π-π interactions with PFAS. Surface changes can improve selectivity and capacity [279]. CNTs, like GO, are expensive to produce, and their aggregation in water can degrade performance [278]. Unresolved problems include their environmental safety, persistence,

and the ability to recover and reuse CNTs following PFAS adsorption.

AHC, especially when made from waste biomass, is emerging as a potential and environmentally friendly alternative. AHC may effectively remove PFAS, especially when activation settings are tuned to enhance surface area and alter surface chemistry. However, its effectiveness is largely reliant on the feedstock and activation technique, resulting in variable adsorption efficiency [276,278]. Regeneration and safe disposal of PFAS-laden hydrochar remain unexplored, and large-scale, standardised manufacturing techniques are currently being developed.

BC is appealing for its inexpensive cost, widespread availability, and environmental advantages. However, unmodified BC usually has poor PFAS adsorption, especially for short-chain compounds and in the presence of NOM [278]. Surface functionalisation (e.g., oxidation, metal doping, or surfactant modification) can greatly increase performance; nevertheless, such alterations raise problems regarding stability, additive leaching, and consistent quality control [6,278].

5.9. Prospects of carbon-based absorbents for PFAS removal

GAC improvements focus on increasing adsorption capacity for SC-PFAS, which typically have low affinity for GAC. Recent improvements include surface modification approaches that boost positive surface charge and modify pore architecture to better collect these difficult chemicals [269]. Innovative regeneration technologies, such as modified supercritical CO_2 extraction, have shown promise in successfully desorbing PFAS from wasted GAC under moderate circumstances [266]. This allows for numerous cycles to be reused without compromising adsorbent characteristics. On-site regeneration solutions are also being developed to cut transportation and disposal costs, save downtime, and assure the responsible destruction of PFAS-laden waste streams, therefore addressing environmental justice issues.

Future research on GO will focus on improving scalability and dispersion stability in aqueous conditions to enhance effective surface area for adsorption [276]. Functionalisation techniques that add to binding sites or improve hydrophilicity are being investigated to boost selectivity and capacity for a wider range of PFAS compounds, including short-chain versions. Research is also concentrating on incorporating GO into composite materials to promote recovery and reuse, hence decreasing environmental problems and toxicity.

CNTs are being developed with a focus on low-cost production and surface engineering to customise adsorption capabilities. Surface changes, such as oxidation or polymer grafting, can increase dispersibility and add functional groups that facilitate PFAS binding [279]. Combining CNTs with additional materials to create hybrid adsorbents may increase mechanical stability and regeneration. Addressing environmental safety and recovery problems remains a top focus for wider use.

AHC development is centred on standardising manufacturing processes to ensure uniform quality and improving activation conditions to enhance surface area and functional group density [276]. Tailoring surface chemistry to enhance interactions with both long- and SC-PFAS is a key goal. Furthermore, combining AHC adsorption with catalytic or hydrothermal degradation processes provides a viable approach for simultaneous PFAS removal and destruction, which improves overall treatment efficacy and sustainability.

Future advances to BC include enhanced surface functionalisation techniques such as metal doping, oxidation, and surfactant coating to considerably increase PFAS adsorption, particularly for short-chain chemicals and complicated water matrices comprising natural organic matter. BC is also being investigated for use in multi-stage treatment trains and composite materials to maximise

synergistic benefits. Another major area of attention is increasing output while ensuring environmental safety and cost-effectiveness [10,276].

6. Conclusions

For the removal of PFAS from water environments, carbon-based adsorption is a vital and successful technique. The adaptability of adsorption materials, including BC, GO, AHC, CNTs and AC, provides a multitude of choices for tackling the problems related to PFAS pollution. These materials are appropriate for both passive and active remediation procedures since they may be modified in many ways to improve their selectivity and adsorption effectiveness. Adsorption-based remediation methods are appealing solutions because of their scalability, low cost, and ecologically benign nature. Adsorbent material optimisation, the creation of novel treatment methods, and an overall increase in the effectiveness of PFAS removal are essential for advancing this field of study.

Adsorption will continue to be a vital part of the toolset in the fight against PFAS pollution and in guaranteeing a more secure and healthy environment for coming generations because of researchers' efforts. For these reasons, the current review presents a discussion of a myriad of adsorbents and their sorption process for PFAS removal. To remove PFASs, the distinguishing characteristics of BC, AHC, GAC, CNTs, and GO are explained. Herein, this research begins by discussing the sources, classes, properties, fate, exposure pathways, toxicological implications, and the traditional detection and quantification methods of PFAS. This review also provides researchers with a clear and comprehensive overview of the current state of PFAS adsorption research by discussing the adsorption mechanisms and theories. Besides, carbon-based materials and PFAS interact synergistically through a mix of hydrophobic forces, electrostatic attraction, hydrogen bonding, and physical entrapment inside porous structures. Improving these interactions by material engineering, such as surface modification, doping, or hybridisation, offers a possible approach to more effective PFAS cleanup methods that can target both historical and new chemicals. Furthermore, the study contributes to the current body of knowledge by suggesting and explaining practical modification options tailored to capture low-molecular-weight, S-C PFAS. By moving the focus from classical hydrophobic partitioning to electrostatic-driven design, revealing cationic functionalisation and metal oxide doping as critical approaches for overcoming short-chain compounds' water mobility. Functional group analysis, linkage of molecular structure to adsorption potential, comparison of carbon-based materials for adsorption, and practical cases and techniques for regeneration and reuse of the five carbon-based materials have all been discussed. The review concludes by discussing the various challenges associated with the adsorbents for the removal of PFASSs and the current and future research directions for enhancing their efficiency, stability and eco-friendliness.

Use of AI tools declaration

The authors declare they have not used Artificial Intelligence (AI) tools in the creation of this article.

Acknowledgments

The authors express thanks to Birmingham City University, College of Engineering, for providing access to essential literature resources.

Conflict of interest

The authors declare that they have no known competing financial interests or personal relationships that could have appeared to influence the work reported in this paper.

Author contributions

Josephine Baffoe: Writing-Original Draft, Resource, Methodology, Investigation, Data Curation; Eliasu Issaka: Conceptualisation, Methodology, Investigation, Data Curation, Resources, Validation, Formal analysis, Writing-Original Draft, Writing-Review and Editing, Supervision, Resources; Eric Danso-Boateng: Writing-Original Draft, Writing-Review and Editing, Resource

References

1. Manojkumar Y, Pilli S, Rao P V, et al. (2023) Sources, occurrence and toxic effects of emerging per- and polyfluoroalkyl substances (PFAS). *Neurotoxicol Teratol* 97: 107174. https://doi.org/10.1016/j.ntt.2023.107174
2. Wang Y, Munir U, Huang Q (2023) Occurrence of per- and polyfluoroalkyl substances (PFAS) in soil: Sources, fate, and remediation. *Soil Environ Health* 1: 100004. https://doi.org/10.1016/j.seh.2023.100004
3. God'sgift N C, Alqattan Z A, Jones M, et al. (2024) Toxic layering and compound extremes: Per- and polyfluoroalkyl substances (PFAS) exposure in rural, environmental justice copper mining communities. *Sci Total Environ* 957: 177767. https://doi.org/10.1016/j.scitotenv.2024.177767
4. Bayode A A, Emmanuel S S, Akinyemi A O, et al. (2024) Innovative techniques for combating a common enemy forever chemicals: A comprehensive approach to mitigating per- and polyfluoroalkyl substances (PFAS) contamination. *Environ Res* 261: 119719. https://doi.org/10.1016/j.envres.2024.119719
5. Murray C C, Vatankhah H, McDonough C A, et al. (2019) Removal of per- and polyfluoroalkyl substances using super-fine powder activated carbon and ceramic membrane filtration. *J Hazard Mater* 366: 160–168. https://doi.org/10.1016/j.jhazmat.2018.11.050
6. Issaka E, Fapohunda F O, Amu-Darko J N O, et al. (2022) Biochar-based composites for remediation of polluted wastewater and soil environments: Challenges and prospects. *Chemosphere* 297: 134163. https://doi.org/10.1016/j.chemosphere.2022.134163
7. Ates M, Eker AA, Eker B (2017) Carbon nanotube-based nanocomposites and their applications. *J Adhes Sci Technol* 31: 1977–1997. https://doi.org/10.1080/01694243.2017.1295625
8. Chen F, Chen J, Liu X, et al. (2024) Removal of per- and polyfluoroalkyl substances by activated hydrochar derived from food waste: Sorption performance and desorption hysteresis. *Environ Pollut* 340: 122820. https://doi.org/10.1016/j.envpol.2023.122820
9. Borane N, Boddula R, Odedara N, et al. (2024) Comprehensive review on synthetic methods and functionalization of graphene oxide: Emerging Applications. *Nano-Structures Nano-Objects* 39: 101282. https://doi.org/10.1016/j.nanoso.2024.101282
10. Issaka E, Adams M, Baffoe J, et al. (2024) Covalent organic frameworks: a review of synthesis methods, properties and applications for per- and poly-fluoroalkyl substances removal. *Clean Technol Environ Policy* 27: 833–860. https://doi.org/10.1007/s10098-024-03102-8

11. Park M, Wu S, Lopez I J, et al. (2020) Adsorption of perfluoroalkyl substances (PFAS) in groundwater by granular activated carbons: Roles of hydrophobicity of PFAS and carbon characteristics. *Water Res* 170: 115364. https://doi.org/10.1016/j.watres.2019.115364
12. Omo-Okoro P N, Curtis C J, Marco A M, et al. (2021) Removal of per- and polyfluoroalkyl substances from aqueous media using synthesized silver nanocomposite-activated carbons. *J Environ Health Sci Eng* 19: 217–236. https://doi.org/10.1007/s40201-020-00597-3
13. Liu Z, Peldszus S, Sauvé S, et al. (2024) Enhanced removal of trace-level per- and polyfluoroalkyl substances (PFAS) from drinking water using granular activated carbon (GAC): The role of ozonation. *Chemosphere* 368: 143758. https://doi.org/10.1016/j.chemosphere.2024.143758
14. Yin S, López J F, Solís J J C, et al. (2023) Enhanced adsorption of PFOA with nano MgAl2O4@CNTs: influence of pH and dosage, and environmental conditions. *J Hazard Mater Adv* 9: 100252. https://doi.org/10.1016/j.hazadv.2023.100252
15. Liu N, Li Y, Zhang M, et al. (2024) Efficient adsorption of short-chain perfluoroalkyl substances by pristine and Fe/Cu-loaded reed straw biochars. *Sci Total Environ* 946: 174223. https://doi.org/10.1016/j.scitotenv.2024.174223
16. Miserli K, Boti V, Konstantinou I (2024) Analysis of perfluorinated compounds in sewage sludge and hydrochar by UHPLC LTQ/Orbitrap MS and removal assessment during hydrothermal carbonization treatment. *Sci Total Environ* 929: 172650. https://doi.org/10.1016/j.scitotenv.2024.172650
17. Sadia M, Nollen I, Helmus R, et al. (2023) Occurrence, Fate, and Related Health Risks of PFAS in Raw and Produced Drinking Water. *Environ. Sci Technol* 57: 3062–3074. https://doi.org/10.1021/acs.est.2c06015
18. Koskue V, Monetti J, Rossi N, et al. (2022) Fate of pharmaceuticals and PFASs during the electrochemical generation of a nitrogen-rich nutrient product from real reject water. *J Environ Chem Eng* 10: 107284. https://doi.org/10.1016/j.jece.2022.107284
19. Rekik H, Arab H, Pichon L, et al. (2024) Per-and polyfluoroalkyl (PFAS) eternal pollutants: Sources, environmental impacts and treatment processes. *Chemosphere* 358: 142044. https://doi.org/10.1016/j.chemosphere.2024.142044
20. Bajpai P (2015) Pulp and Paper Chemicals. *Pulp and Paper Industry* 103–106. https://doi.org/10.1016/B978-0-12-803409-5.00008-2
21. Anik A H, Basir M S, Sultan M B, et al. (2025) Unveiling the emerging concern of per- and polyfluoroalkyl substances (PFAS) and their potential impacts on estuarine ecosystems. *Mar Pollut Bull* 212: 117554. https://doi.org/10.1016/j.marpolbul.2025.117554
22. Reinikainen J, Perkola N, Äystö L, et al. (2022) The occurrence, distribution, and risks of PFAS at AFFF-impacted sites in Finland. *Sci Total Environ* 829: 154237. https://doi.org/10.1016/j.scitotenv.2022.154237
23. Behroozi A H, Meunier L, Mirahsani A, et al. (2025) Graphene-based materials and technologies for the treatment of PFAS in water: A review of recent developments. *J Hazard Mater Adv* 17: 100626. https://doi.org/10.1016/j.hazadv.2025.100626
24. Issaka E, Adams M, Agyekum E A, et al. (2025) Per- and poly-fluoroalkyl substances: A review of sources, properties, chromatographic detection, and toxicological implications. *AIMS Environ Sci* 12: 321–351. https://doi.org/10.3934/environsci.2025015

25. McCord J, Strynar M (2019) Identification of Per- and Polyfluoroalkyl Substances in the Cape Fear River by High Resolution Mass Spectrometry and Nontargeted Screening. *Environ Sci Technol* 53: 4717–4727. https://doi.org/10.1021/acs.est.8b06017
26. Duan Y, Sun H, Yao Y, et al. (2020) Distribution of novel and legacy per-/polyfluoroalkyl substances in serum and its associations with two glycemic biomarkers among Chinese adult men and women with normal blood glucose levels. *Environ Int* 134: 105295. https://doi.org/10.1016/j.envint.2019.105295
27. Liu J, Cui Y, Lu M, et al. (2022) 6:2 Chlorinated polyfluoroalkyl ether sulfonate as perfluorooctanesulfonate alternative in the electroplating industry and the receiving environment. *Chemosphere* 302: 105295. https://doi.org/10.1016/j.chemosphere.2022.134719
28. Brendel S, Fetter É, Staude C, et al. (2018) Short-chain perfluoroalkyl acids: environmental concerns and a regulatory strategy under REACH. *Environ Sci Eur* 30: 9. https://doi.org/10.1186/s12302-018-0134-4
29. Valencia A, Ordonez D, Sadmani A H M A, et al. (2023) Comparing the removal and fate of long and short chain per- and polyfluoroalkyl substances (PFAS) during surface water treatment via specialty adsorbents. *J Water Process Eng* 56: 104345. https://doi.org/10.1016/j.jwpe.2023.104345
30. Riegel M, Haist-Gulde B, Sacher F (2023) Sorptive removal of short-chain perfluoroalkyl substances (PFAS) during drinking water treatment using activated carbon and anion exchanger. *Environ Sci Eur* 35: 12. https://doi.org/10.1186/s12302-023-00716-5
31. Chambial P, Thakur N, Kushawaha J, et al. (2025) Per- and polyfluoroalkyl substances in environment and potential health impacts: Sources, remediation treatment and management, policy guidelines, destructive technologies, and techno-economic analysis. *Sci Total Environ* 969: 178803. https://doi.org/10.1016/j.scitotenv.2025.178803
32. Androulakakis A, Alygizakis N, Bizani, E, et al. (2022) Current progress in the environmental analysis of poly- and perfluoroalkyl substances (PFAS). *Environ Sci Adv* 1: 705–724. https://doi.org/10.1039/D2VA00147K
33. Bhardwaj S, Lee M, O'Carroll D, et al. (2024) Biotransformation of 6:2/4:2 fluorotelomer alcohols by Dietzia aurantiaca J3: Enzymes and proteomics. *J Hazard Mater* 478: 135510. https://doi.org/10.1016/j.jhazmat.2024.135510
34. Umeh OR, Ibo EM, Eke CI, et al. (2025) Out of sight, into the spotlight: Beyond the current state of science on per- and poly-fluoroalkyl substances in groundwater. *J Environ Manage* 373: 123941. https://doi.org/10.1016/j.jenvman.2024.123941
35. Yuan W, Song S, Lu Y, et al. (2024) Legacy and alternative per-and polyfluoroalkyl substances (PFASs) in the Bohai Bay Rim: Occurrence, partitioning behavior, risk assessment, and emission scenario analysis. *Sci Total Environ* 912: 168837. https://doi.org/10.1016/j.scitotenv.2023.168837
36. Cheng Y, Hu Y, Yu K, et al. (2024) Occurrence of legacy and Emerging per- and polyfluoroalkyl substances (PFASs) in indoor dust from office environment in south china. *Emerg Contam* 10: 100375. https://doi.org/10.1016/j.emcon.2024.100375
37. Wang Y, Xie J, Ren Z, et al. (2022) Postsynthetically modified hydrophobic covalent organic frameworks for enhanced oil/water and CH4/C2H2 separation. *Chem Eng J* 448: 137687. https://doi.org/10.1016/j.cej.2022.137687

38. Usuda H, Mishima Y, Noda K, et al. (2024) Vesicles exhibit high-performance removal of per- and polyfluoroalkyl substances (PFAS) depending on their hydrophobic groups. *Chemosphere* 363: 142818. https://doi.org/10.1016/j.chemosphere.2024.142818
39. Zhang X, Liu J, Zhang H, et al. (2025) Highly selective guanidine-linked covalent organic framework for efficient removal of perfluoroalkyl carboxylic acids from water samples. *Sep Purif Technol* 357: 130039. https://doi.org/10.1016/j.seppur.2024.130039
40. Ruan G, Yang Y, Peng X, et al. (2025) A review of the current status of nitrogen self-doped biochar applications. *J Environ Chem Eng* 13: 115291. https://doi.org/10.1016/j.jece.2024.115291
41. Brown-Leung JM, Cannon JR (2022) Neurotransmission Targets of Per- and Polyfluoroalkyl Substance Neurotoxicity: Mechanisms and Potential Implications for Adverse Neurological Outcomes. *Chem Res Toxicol* 35: 1312. https://doi.org/10.1021/acs.chemrestox.2c00072
42. Leung SCE, Wanninayake D, Chen D, et al. (2023) Physicochemical properties and interactions of perfluoroalkyl substances (PFAS) - Challenges and opportunities in sensing and remediation. *Sci Total Environ* 905: 166764. https://doi.org/10.1016/j.scitotenv.2023.166764
43. Gao Y, Tang P, Zhou H, et al. (2016) Graphene Oxide Catalyzed C-H Bond Activation: The Importance of Oxygen Functional Groups for Biaryl Construction. *Angew Chem Int Ed Engl* 55: 3124–3128. https://doi.org/10.1002/anie.201510081
44. Ellis DA, Martin JW, De Silva AO, et al. (2004) Degradation of Fluorotelomer Alcohols: A Likely Atmospheric Source of Perfluorinated Carboxylic Acids. *Environ Sci Technol* 38: 3316–3321. https://doi.org/10.1021/es049860w
45. Bere K, Bakk B, Illés E, et al. (2024) Role of Fluorocarbon Chain Length in the Adsorption of Perfluoroalkyl Substances on Nanoplastic Particles. *ACS ES&T Water* 4: 5114–5121. https://doi.org/10.1021/acsestwater.4c00689
46. Wang Y, Darling SB, Chen J (2021) Selectivity of Per- and Polyfluoroalkyl Substance Sensors and Sorbents in Water. *ACS Appl Mater Interfaces* 13: 60789–60814. https://doi.org/10.1021/acsami.1c16517
47. Behnami A, Pourakbar M, Ayyar ASR, et al. (2024) Treatment of aqueous per- and poly-fluoroalkyl substances: A review of biochar adsorbent preparation methods. *Chemosphere* 357: 142088. https://doi.org/10.1016/j.chemosphere.2024.142088
48. Chen J, Samaei SHA, Zhang L, et al. (2025) Per- and poly-fluoroalkyl substances (PFAS) in water matrices impacted by industrial activities: Challenges and treatment strategies. *J Hazard Mater Adv* 20: 100920. https://doi.org/10.1016/j.hazadv.2025.100920
49. Zhou D, Zhang C, Li L, et al. (2025) Grafting quaternary ammonium onto polyvinyl alcohol for imparting durable antibacterial, flame-retardant, and recyclable anion-absorptive properties. *Polymer* 336: 128939. https://doi.org/10.1016/j.polymer.2025.128939
50. Su H, Gao P, Wang MY, et al. (2018) Grouping Effect of Single Nickel-N4 Sites in Nitrogen-Doped Carbon Boosts Hydrogen Transfer Coupling of Alcohols and Amines. *Angew Chem Int Ed Engl* 57: 15194–15198. https://doi.org/10.1002/anie.201809858
51. Zhao S, Li ZX, Guo HT, et al. (2025) Critical Role of Carbon Substrates in Optimizing Ru-Based HER Catalysts: From Dimensional Insights to Metal-Support Interactions Engineering. *Adv Funct Mater* 36: e09799. https://doi.org/10.1002/adfm.202509799

52. Solan TDE, Saleh NM, Begum S, et al. (2025) Ultra-high selective adsorbents for per- and polyfluoroalkyl substances (PFAS) destruction: Bridging the gap between adsorption and catalytic degradation for excellent performance in persistent environmental contaminants. *Results Eng* 28: 107901. https://doi.org/10.1016/j.rineng.2025.107901
53. Du Y, Cai Y, Teng L, et al. (2026) Fabrication and applications of ionic covalent organic framework membranes. *J Mater Chem A Mater* 14: 3719–3770. https://doi.org/10.1039/D5TA06080J
54. Akinnawo SO (2024) Per- and polyfluoroalkyl substances sequestration by adsorption and photocatalysis: Technical challenges and pragmatic solution. *Desalin Water Treat* 319: 100437. https://doi.org/10.1016/j.dwt.2024.100437
55. Song Z, He J, Kouzehkanan SMT, et al. (2024) Enhanced sorption and destruction of PFAS by biochar-enabled advanced reduction process. *Chemosphere* 363: 142760. https://doi.org/10.1016/j.chemosphere.2024.142760
56. Gautam RK, Mottaghipisheh J, Verma S, et al. (2025) PFAS contamination in key indian states: A critical review of environmental impacts, regulatory challenges and predictive exposure. *J Hazard Mater Adv* 18: 100748. https://doi.org/10.1016/j.hazadv.2025.100748
57. Peng X, Yang Y, Wang J, et al. (2023) Cu/Fe co-modified nitrogen self-doped biochar as a heterogeneous Fenton-like catalyst for degradation of organic pollutants: Synthesis, performance, and mechanistic study. *J Environ Chem Eng* 11: 110866. https://doi.org/10.1016/j.jece.2023.110866
58. Kundu S, Khandaker T, Anik MAAM, et al. (2024) A comprehensive review of enhanced CO2 capture using activated carbon derived from biomass feedstock. *RSC Adv* 14: 29693. https://doi.org/10.1039/D4RA04537H
59. Ma X, Yuan H, Hu M (2019) A simple method for synthesis of ordered mesoporous carbon. *Diam Relat Mater* 98: 107480. https://doi.org/10.1016/j.diamond.2019.107480
60. Walkowiak-Kulikowska J (2022) Poly/Perfluorinated Alkyl Substances (PFASs)–Synthetic Methods, Properties and Applications. https://doi.org/10.1039/9781839167591-00022
61. Li X, Shen H, Pan X, et al. (2025) Kinetic study of the fluoride removal by gypsum using revised pseudo-second-order model: Insights on the surface adsorption and precipitation. *Surf Interfaces* 62. https://doi.org/10.1016/j.surfin.2025.106304
62. Phong Vo HN, Ngo HH, Guo W, et al. (2020) Poly-and perfluoroalkyl substances in water and wastewater: A comprehensive review from sources to remediation. *Environ Pollut* 36: 101393. https://doi.org/10.1016/j.jwpe.2020.101393
63. Taliantzis K, Ellinas K (2025) Green hydrophobic and superhydrophobic coatings and surfaces for water related applications: A review. *Adv Colloid Interface Sci* 343: 103566. https://doi.org/10.1016/j.cis.2025.103566
64. Choi YJ, Helbling DE, Liu J, et al. (2022) Microbial biotransformation of aqueous film-forming foam derived polyfluoroalkyl substances. *Sci Total Environ* 824: 15371. https://doi.org/10.1016/j.scitotenv.2022.153711
65. Kang KH, Saifuddin M, Chon K, et al. (2024) Recent advances in the application of magnetic materials for the management of perfluoroalkyl substances in aqueous phases. *Chemosphere* 352: 141522. https://doi.org/10.1016/j.chemosphere.2024.141522

66. Chow YN, Foo KY (2023) Insights into the per- and polyfluoroalkyl substances-contaminated paper mill processing discharge: Detection, phytotoxicity, bioaccumulative profiling, and health risk verification. *J Clean Prod* 384: 135478. https://doi.org/10.1016/j.jclepro.2022.135478
67. Hanvoravongchai J, Laochindawat M, Kimura Y, et al. (2024) Clinical, histological, molecular, and toxicokinetic renal outcomes of per-/polyfluoroalkyl substances (PFAS) exposure: Systematic review and meta-analysis. *Chemosphere* 368: 143745. https://doi.org/10.1016/j.chemosphere.2024.143745
68. Modiri M, Sasi PC, Thompson KA, et al. (2024) State of the science and regulatory acceptability for PFAS residual management options: PFAS disposal or destruction options. *Chemosphere* 368: 143726. https://doi.org/10.1016/j.chemosphere.2024.143726
69. Kali SE, Österlund H, Viklander M, et al. (2025) Stormwater discharges affect PFAS occurrence, concentrations, and spatial distribution in water and bottom sediment of urban streams. *Water Res* 271: 122973. https://doi.org/10.1016/j.watres.2024.122973
70. Ohoro CR, Amaku JF, Conradie J, et al. (2024) Effect of physicochemical parameters on the occurrence of per- and polyfluoroalkyl substances (PFAS) in aquatic environment. *Mar Pollut Bull* 208: 17040. https://doi.org/10.1016/j.marpolbul.2024.117040
71. Zhou Y, Wang X, Wang C, et al. (2024) Fate of 'forever chemicals' in the global cryosphere. *Earth Sci Rev* 259: 104973. https://doi.org/10.1016/j.earscirev.2024.104973
72. Jaskulak M, Zimowska M, Rolbiecka M, et al. (2025) Understanding the role of endocrine disrupting chemicals as environmental obesogens in the obesity epidemic: A comprehensive overview of epidemiological studies between 2014 and 2024. *Ecotoxicol Environ Saf* 299: 118401. https://doi.org/10.1016/j.ecoenv.2025.118401
73. Rupp J, Guckert M, Berger U, et al. (2023) Comprehensive target analysis and TOP assay of per- and polyfluoroalkyl substances (PFAS) in wild boar livers indicate contamination hot-spots in the environment. *Sci Total Environ* 871. https://doi.org/10.1016/j.scitotenv.2023.162028
74. Gerardu T, Dijkstra J, Beeltje H, et al. (2023) Accumulation and transport of atmospherically deposited PFOA and PFOS in undisturbed soils downwind from a fluoropolymers factory. *Environ Adv* 11: 100332. https://doi.org/10.1016/j.envadv.2022.100332
75. Dhiman S, Jain HV, Yadav A, et al. (2025) Probing the fate and transport of PFAS in urban soils: Insights from ASE-LC-HR/MS analysis. *J Hazard Mater* 494: 138635. https://doi.org/10.1016/j.jhazmat.2025.138635
76. Moavenzadeh Ghaznavi S, Flores Azua AJ, Kopec AD, et al. (2024) Permeation of per- and polyfluoroalkyl substances (PFAS)-laden leachate in landfills as an outcome of puncture failures of high-density polyethylene geomembranes. *Environ Pollut* 363: 125234. https://doi.org/10.1016/j.envpol.2024.125234
77. Liu Y, Samarasinghe SC, Wijayawardena MA, et al. (2025) PFAS soil contamination and remediation. *Treatise on Geochemistry, Third Edition,* 8: 35–63. https://doi.org/10.1016/B978-0-323-99762-1.00047-4
78. Dauchy X, Boiteux V, Bach C, et al. (2017) Per- and polyfluoroalkyl substances in firefighting foam concentrates and water samples collected near sites impacted by the use of these foams. *Chemosphere* 183: 53–61. https://doi.org/10.1016/j.chemosphere.2017.05.056

79. Witt CC, Gadek CR, Cartron JLE, et al. (2024) Extraordinary levels of per- and polyfluoroalkyl substances (PFAS) in vertebrate animals at a New Mexico desert oasis: Multiple pathways for wildlife and human exposure. *Environ Res* 249: 18229. https://doi.org/10.1016/j.envres.2024.118229
80. Hassan MT Al, Chen X, Fnu PIJ, et al. (2024) Rapid detection of per- and polyfluoroalkyl substances (PFAS) using paper spray-based mass spectrometry. *J Hazard Mater* 465: 133366. https://doi.org/10.1016/j.jhazmat.2023.133366
81. Pinney SM, Biro FM, Fassler CS, et al. (2023) Exposure to Perfluoroalkyl Substances and Associations with Pubertal Onset and Serum Reproductive Hormones in a Longitudinal Study of Young Girls in Greater Cincinnati and the San Francisco Bay Area. *Environ Health Perspect* 131. https://doi.org/10.1289/EHP11811
82. Marumure J, Simbanegavi TT, Makuvara Z, et al. (2024) Emerging organic contaminants in drinking water systems: Human intake, emerging health risks, and future research directions. *Chemosphere* 356: 141699. https://doi.org/10.1016/j.chemosphere.2024.141699
83. Jiang Z, Li X, Wang R, et al. (2025) Extraction performance of SiO2@COF before and after carbonization and online SPE-HPLC-DAD methods for tetrabromobisphenol A derivatives and phthalates. *Talanta* 285: 127285. https://doi.org/10.1016/j.talanta.2024.127285
84. Morgan S, Raza Shah SH, Comstock SS, et al. (2025) Prenatal PFAS exposure and outcomes related to maternal gut microbiome composition in later pregnancy. *Environ Res* 279: 121709. https://doi.org/10.1016/j.envres.2025.121709
85. Abuduxukuer K, Wang H, Wang C, et al. (2025) Prenatal exposure to per-and polyfluoroalkyl substances and its association with Developmental Defects of Enamel (DDE) and dental caries in 4 years old children: Findings from Shanghai birth cohort. *Environ Int* 198: 109411. https://doi.org/10.1016/j.envint.2025.109411
86. Abioye KJ, Harun NY, Yusuf M, et al. (2024) RSM-based co-gasification of palm oil decanter cake and sugarcane bagasse: Syngas production and biochar characteristics. *Biomass Bioenerg* 191: 10748. https://doi.org/10.1016/j.biombioe.2024.107482
87. Rajan AK, Mohanty A, Swain P, et al. (2025) Cell-free circulating epigenomic signatures: Non-invasive biomarkers of pregnancy-related outcomes associated with plasticizer exposure. *Reprod Toxicol* 137: 109000. https://doi.org/10.1016/j.reprotox.2025.109000
88. Pande A, Kinkade CW, Prout N, et al. (2024) Prenatal exposure to synthetic chemicals in relation to HPA axis activity: A systematic review of the epidemiological literature. *Sci Total Environ* 956: 177300. https://doi.org/10.1016/j.scitotenv.2024.177300
89. Cai Z, Zhou G, Yu X, et al. (2025) Perfluorooctanoic acid disrupts thyroid hormone biosynthesis by altering glycosylation of Na+/I− symporter in larval zebrafish. *Ecotoxicol Environ Saf* 297: 118249. https://doi.org/10.1016/j.ecoenv.2025.118249
90. Pan Z, Miao W, Wang C, et al. (2021) 6:2 Cl-PFESA has the potential to cause liver damage and induce lipid metabolism disorders in female mice through the action of PPAR-γ. *Environ Pollut* 287: 117329. https://doi.org/10.1016/j.envpol.2021.117329
91. Cohn BA, La Merrill MA, Krigbaum NY, et al. (2020) In utero exposure to poly− and perfluoroalkyl substances (PFASs) and subsequent breast cancer. *Reprod Toxicol* 92: 112–119. https://doi.org/10.1016/j.reprotox.2019.06.012

92. Furlong MA, Liu T, Jung A, et al. (2025) Per- and polyfluoroalkyl substances (PFAS) and microRNA: An epigenome-wide association study in firefighters. *Environ Res* 279: 121766. https://doi.org/10.1016/j.envres.2025.121766
93. Pesonen M, Vähäkangas K (2024) Involvement of per- and polyfluoroalkyl compounds in tumor development. *Arch Toxicol* 98: 1241. https://doi.org/10.1007/s00204-024-03685-7
94. Chaudhary A, Bashir W, Majid A, et al. (2025) PFAS insights: A review of historical data, environmental applications, health effects, and pollution challenges in Pakistan. *Environ Sci Policy* 167: 104056. https://doi.org/10.1016/j.envsci.2025.104056
95. Ansell GK, Javed H (2025) PFAS Analytical Methods – A Practical Guide. *J Fluor Chem* 285: 110444. https://doi.org/10.1016/j.jfluchem.2025.110444
96. Stroski KM, Sapozhnikova Y (2025) Method development and validation for analysis of 74 per- and polyfluoroalkyl substances (PFAS) in food of animal origin using QuEChERSER method and LC-MS/MS. *Anal Chim Acta* 1364: 344216. https://doi.org/10.1016/j.aca.2025.344216
97. Sapozhnikova Y, Stroski K (2025) Analysis of neutral per- and polyfluoroalkyl substances (PFAS) by gas chromatography – high resolution mass spectrometry (GC[sbnd]HRMS). *J Chromatogr A* 1753: 465989. https://doi.org/10.1016/j.chroma.2025.465989
98. Di Giorgi A, Basile G, Bertola F, et al. (2024) A green analytical method for the simultaneous determination of 17 perfluoroalkyl substances (PFAS) in human serum and semen by ultra-performance liquid chromatography-tandem mass spectrometry (UPLC-MS/MS). *J Pharm Biomed Anal* 246: 116203. https://doi.org/10.1016/j.jpba.2024.116203
99. Badawy MEI, El-Nouby MAM, Kimani PK, et al. (2022) A review of the modern principles and applications of solid-phase extraction techniques in chromatographic analysis. *Analytical Sciences* 38: 1457–1487. https://doi.org/10.1007/s44211-022-00190-8
100. Mertens H, Noll B, Schwerdtle T, et al. (2023) Less is more: a methodological assessment of extraction techniques for per- and polyfluoroalkyl substances (PFAS) analysis in mammalian tissues. *Anal Bioanal Chem* 415: 5925–5938. https://doi.org/10.1007/s00216-023-04867-5
101. Nassazzi W, Lai FY, Ahrens L (2022) A novel method for extraction, clean-up and analysis of per- and polyfluoroalkyl substances (PFAS) in different plant matrices using LC-MS/MS. *J Chromatogr B* 1212: 123514. https://doi.org/10.1016/j.jchromb.2022.123514
102. Chiumiento F, Bellocci M, Ceci R, D'Antonio, et al. (2023) A new method for determining PFASs by UHPLC-HRMS (Q-Orbitrap): Application to PFAS analysis of organic and conventional eggs sold in Italy. *Food Chem* 401: 134135. https://doi.org/10.1016/j.foodchem.2022.134135
103. Nazim T, Lusina A, Cegłowski M (2023) Recent Developments in the Detection of Organic Contaminants Using Molecularly Imprinted Polymers Combined with Various Analytical Techniques. *Polymers* 15: 3868. https://doi.org/10.3390/polym15193868
104. Mahinroosta R, Senevirathna L (2020) A review of the emerging treatment technologies for PFAS contaminated soils. *J Environ Manage* 255: 109896. https://doi.org/10.1016/j.jenvman.2019.109896
105. Liu L, Che N, Wang S, et al. (2021) Copper Nanoparticle Loading and F Doping of Graphene Aerogel Enhance Its Adsorption of Aqueous Perfluorooctanoic Acid. *ACS Omega* 6: 7073–7085. https://doi.org/10.1021/acsomega.1c00044
106. Wu J, Fu X, Zhao L, et al. (2024) Biochar as a partner of plants and beneficial microorganisms to assist in-situ bioremediation of heavy metal contaminated soil. *Sci Total Environ* 923: 171442. https://doi.org/10.1016/j.scitotenv.2024.171442

107. Buss W, Wurzer C, Bach M, et al. (2022) Highly efficient phosphorus recovery from sludge and manure biochars using potassium acetate pre-treatment. *J Environ Manage* 314: 15035. https://doi.org/10.1016/j.jenvman.2022.115035
108. Wang J, Chen S, Xu JY, et al. (2021) High-surface-area porous carbons produced by the mild KOH activation of a chitosan hydrochar and their CO2 capture. *Xinxing Tan Cailiao/New Carbon Materials* 36: 1081–1093. https://doi.org/10.1016/S1872-5805(21)60074-4
109. Jalilian M, Bissessur R, Ahmed M, et al. (2024) A review: Hydrochar as potential adsorbents for wastewater treatment and CO2 adsorption. *Sci Total Environ* 914. https://doi.org/10.1016/j.scitotenv.2023.169823
110. Lei X, Lian Q, Zhang X, et al. (2023) A review of PFAS adsorption from aqueous solutions: Current approaches, engineering applications, challenges, and opportunities. *Environ Pollut* 321. https://doi.org/10.1016/j.envpol.2023.121138
111. Dey D, Shafi T, Chowdhury S, et al. (2024) Progress and perspectives on carbon-based materials for adsorptive removal and photocatalytic degradation of perfluoroalkyl and polyfluoroalkyl substances (PFAS). *Chemosphere* 351: 141164. https://doi.org/10.1016/j.chemosphere.2024.141164
112. Mahpishanian S, Zhou M, Foudazi R (2024) Magnetic amino-functionalized graphene oxide nanocomposite for PFAS removal from water. *Environ Sci Adv* 3: 1698–1713. https://doi.org/10.1039/D4VA00171K
113. Mahanty B, Saawarn B, Mahto B, et al. (2024) Efficient removal of perfluorooctanoic acid from aqueous matrices using cationic surfactant functionalized graphene oxide nanocomposite: RSM and ANN modeling, and adsorption behaviour. *Environ Pollut* 68: 106448. https://doi.org/10.1016/j.jwpe.2024.106448
114. Cantoni B, Turolla A, Wellmitz J, et al. (2021) Perfluoroalkyl substances (PFAS) adsorption in drinking water by granular activated carbon: Influence of activated carbon and PFAS characteristics. *Sci Total Environ* 795. https://doi.org/10.1016/j.scitotenv.2021.148821
115. Burkhardt JB, Cadwallader A, Pressman JG, et al. (2023) Polanyi adsorption potential theory for estimating PFAS treatment with granular activated carbon. *Environ Pollut* 53. https://doi.org/10.1016/j.jwpe.2023.103691
116. Dey D, Chatterjee S (2020) *Biochar: A Useful Amendment for Sustaining Soil Environment*, AkiNik Publications.
117. Jain A, Balasubramanian R, Srinivasan MP (2016) Hydrothermal conversion of biomass waste to activated carbon with high porosity: A review. *Chem Eng J* 283: 789–805. https://doi.org/10.1016/j.cej.2015.08.014
118. Yahyazadeh A, Nanda S, Dalai AK (2024) Carbon Nanotubes: A Review of Synthesis Methods and Applications. *Reactions* 5: 429–451. https://doi.org/10.3390/reactions5030022
119. Sun L (2019) Structure and synthesis of graphene oxide. *Chin J Chem Eng* 27: 2251–2260. https://doi.org/10.1016/j.cjche.2019.05.003
120. Yin Z, Wu F, He C, et al. (2023) Renewable biomass-derived, P-doped granular activated carbon for efficient oxidation of 5-hydroxymethylfurfural to 2,5-diformylfuran: Insights into the crucial role of P and N functionality. *Renew Energy* 219: 119388. https://doi.org/10.1016/j.renene.2023.119388

121. Nomicisio C, Ruggeri M, Bianchi E, et al. (2023) Natural and Synthetic Clay Minerals in the Pharmaceutical and Biomedical Fields. *Pharmaceutics* 15: 1368. https://doi.org/10.3390/pharmaceutics15051368
122. Singh J, Bhattu M, Liew RK, et al. (2024) Transforming rice straw waste into biochar for advanced water treatment and soil amendment applications. *Environ Technol Innov* 103932. https://doi.org/10.1016/j.eti.2024.103932
123. Nasrollahpour S, Tanhadoust A, Pulicharla R, et al. (2024) Long-chain perfluoroalkyl carboxylic acids removal by biochar: Experimental study and uncertainty based data-driven predictive model. *iScience* 27: 111140. https://doi.org/10.1016/j.isci.2024.111140
124. Tasca AL, Puccini M, Gori R, et al. (2019) Hydrothermal carbonization of sewage sludge: A critical analysis of process severity, hydrochar properties and environmental implications. *Waste Management* 93: 1–13. https://doi.org/10.1016/j.wasman.2019.05.027
125. Omari RA, Aung HP, Hou M, Yokoyama, et al. (2016) Influence of Different Plant Materials in Combination with Chicken Manure on Soil Carbon and Nitrogen Contents and Vegetable Yield. *Pedosphere* 26: 510–521. https://doi.org/10.1016/S1002-0160(15)60061-3
126. Cheng J, Islam MT, Sadmani AHMA, et al. (2024) The effect of biochar in a specialty adsorbent on enhanced PFAS removal from surface water. *Environ Pollut* 67: 106231. https://doi.org/10.1016/j.jwpe.2024.106231
127. Ige AR, Łaska G (2025) Production of antioxidant additives and biochar pellets from the Co-pyrolysis of agricultural biomass: A review. *Renewable and Sustainable Energy Reviews* 208. https://doi.org/10.1016/j.rser.2024.115037
128. Ercan B, Alper K, Ucar S, et al. (2023) Comparative studies of hydrochars and biochars produced from lignocellulosic biomass via hydrothermal carbonization, torrefaction and pyrolysis. *Journal of the Energy Institute* 109. https://doi.org/10.1016/j.joei.2023.101298
129. Park S, Kim SJ, Oh KC, et al. (2024) Confirmation of the feasibility of using agrobyproduct biochar in thermal power plants through oxygen pyrolysis and conventional pyrolysis. *J Anal Appl Pyrolysis* 183. https://doi.org/10.1016/j.jaap.2024.106791
130. Bianasari AA, Khaled MS, Hoang TD, et al. (2024) Influence of combined catalysts on the catalytic pyrolysis process of biomass: A systematic literature review. *Energy Convers. Manag* 309. https://doi.org/10.1016/j.enconman.2024.118437
131. Ige AR, Łaska G (2025) Production of antioxidant additives and biochar pellets from the Co-pyrolysis of agricultural biomass: A review. *Renewable and Sustainable Energy Reviews* 208. https://doi.org/10.1016/j.rser.2024.115037
132. Guo L, Lai X, Peng L, et al. (2023) Facile synthesis of Fe and N co-coped biochar from low temperature pyrolysis of lignin waste for superefficient Th(IV)/U(VI) separation: Performance and mechanism. *J Clean Prod* 426: 139168. https://doi.org/10.1016/j.jclepro.2023.139168
133. Handiso B, Pääkkönen T, Wilson BP (2024) Effect of pyrolysis temperature on the physical and chemical characteristics of pine wood biochar. *Waste Management Bulletin* https://doi.org/10.1016/j.wmb.2024.11.008
134. Mishra R, Shu CM, Gollakota ARK, et al. (2024) Unveiling the potential of pyrolysis-gasification for hydrogen-rich syngas production from biomass and plastic waste. *Energy Convers Manag* 321. https://doi.org/10.1016/j.enconman.2024.118997

135. Mu Q, Aleem RD, Liu C, Elendu, et al. (2024) Oxygen blown steam gasification of different kinds of lignocellulosic biomass for the production of hydrogen-rich syngas. *Renew Energy* 232. https://doi.org/10.1016/j.renene.2024.121132
136. Ye S, Hao S, Yan C, et al. (2025) Optimization of microalgal hydrothermal carbonization parameters using the response surface method for biochar applications in blast furnaces to reduce carbon emissions. *Fuel* 381. https://doi.org/10.1016/j.fuel.2024.133671
137. V S, Pillai R, Balan R, et al. (2024) Nanoarchitectonics of hydrothermal carbonized sugarcane juice-derived biochar for high supercapacitance and dye adsorption performance. *Nano-Structures Nano-Objects* 39. https://doi.org/10.1016/j.nanoso.2024.101249
138. Wang H, Xue Y, Hou D, et al. (2025) Hydrothermal co-carbonization of medium-density fiberboard with N-rich compounds to produce N-containing compounds and N-doped biochar: Product distribution, nitrogen transformation pathway and electrochemical performance. *Fuel* 381: 133584. https://doi.org/10.1016/j.fuel.2024.133584
139. Tan M, Li H, Huang Z, et al. (2024) Metal chlorides and ammonium persulfate hydrothermal carbonization for enhanced pyrolysis behavior and biochar properties. *J Anal Appl Pyrolysis* 179: 106469. https://doi.org/10.1016/j.jaap.2024.106469
140. Zaman F, Du Z, Zhao W, et al. (2024) Negatively charged hydrochar from Aesculus indica waste: A sustainable material for enhanced Li-S batteries performance. *Electrochim Acta* 493. https://doi.org/10.1016/j.electacta.2024.144393
141. Fallah S, Alavi N, Tavakoli O, et al. (2023) Optimization of hydrothermal carbonization of food waste as sustainable energy conversion approach: Enhancing the properties of hydrochar by landfill leachate substitution as reaction medium and acetic acid catalyst addition. *Energy Convers. Manag* 297. https://doi.org/10.1016/j.enconman.2023.117647
142. Chen F, Chen J, Liu X, et al. (2024) Removal of per- and polyfluoroalkyl substances by activated hydrochar derived from food waste: Sorption performance and desorption hysteresis. *Environ Pollut* 340: 122820. https://doi.org/10.1016/j.envpol.2023.122820
143. Mujtaba M, Fernandes Fraceto L, Fazeli M, et al. (2023) Lignocellulosic biomass from agricultural waste to the circular economy: a review with focus on biofuels, biocomposites and bioplastics. *J Clean Prod* 402. https://doi.org/10.1016/j.jclepro.2023.136815
144. Azzaz A, Khiari B, Jellali (2020) Hydrochars production, characterization and application for wastewater treatment: A review. *Elsevier*. 127: 109882. https://doi.org/10.1016/j.rser.2020.109882
145. Khoshbouy R, Takahashi F, research KY (2019) Preparation of high surface area sludge-based activated hydrochar via hydrothermal carbonization and application in the removal of basic dye. *Elsevier*. https://doi.org/10.1016/j.envres.2019.04.002
146. Zubbri NA, Mohamed AR, Lahijani P, et al. (2021) Low temperature CO2 capture on biomass-derived KOH-activated hydrochar established through hydrothermal carbonization with water-soaking pre-treatment. *J Environ Chem Eng* 9: 105074. https://doi.org/10.1016/j.jece.2021.105074
147. Ghorbani Gorji S, Hawker DW, Mackie R, et al. (2023) Sorption affinity and mechanisms of per- and polyfluoroalkyl substances (PFASs) with commercial sorbents: Implications for passive sampling. *J Hazard Mater* 457. https://doi.org/10.1016/j.jhazmat.2023.131688

148. Min X, Huo J, Dong Q, et al. (2022) Enhanced sorption of perfluorooctanoic acid with organically functionalized layered double hydroxide. *Chem Eng J* 446: 137019. https://doi.org/10.1016/j.cej.2022.137019
149. Sharma N, Kumar V, Sugumar V, et al. (2024) A comprehensive review on the need for integrated strategies and process modifications for per- and polyfluoroalkyl substances (PFAS) removal: Current insights and future prospects. *Case Stud Chem Environ Eng* 9: 100623. https://doi.org/10.1016/j.cscee.2024.100623
150. Mayakaduwage S, Ekanayake A, Kurwadkar S, et al. (2022) Phytoremediation prospects of per- and polyfluoroalkyl substances: A review. *Environ Res* 212: 113311. https://doi.org/10.1016/j.envres.2022.113311
151. Song XL, Lv H, Liao KC, et al. (2023) Application of magnetic carbon nanotube composite nanospheres in magnetic solid-phase extraction of trace perfluoroalkyl substances from environmental water samples. *Talanta* 253: 123930. https://doi.org/10.1016/j.talanta.2022.123930
152. Aminul Islam M, Hasan M, Rahman M, et al. (2024) Advances and significances of carbon nanotube applications: A comprehensive review. *Eur Polym J* 220: 113443. https://doi.org/10.1016/j.eurpolymj.2024.113443
153. Zakaria MR, Omar MF, Zainol Abidin MS, et al. (2022) Recent progress in the three-dimensional structure of graphene-carbon nanotubes hybrid and their supercapacitor and high-performance battery applications. *Compos. Part A Appl Sci Manuf* 154: 106756. https://doi.org/10.1016/j.compositesa.2021.106756
154. Kolwadkar PM, Acharya NN, Lade VG (2024) Preparation of bio-derived carbon nanostructures by chemical vapor deposition. *Bio-derived Car Nanostruct* 151–179. https://doi.org/10.1016/B978-0-443-13579-8.00003-6
155. Bulla M, Kumar V, Devi R, et al. (2024) Exploring the frontiers of carbon nanotube synthesis techniques and their potential applications in supercapacitors, gas sensing, and water purification. *J Environ Chem Eng* 12: 114504. https://doi.org/10.1016/j.jece.2024.114504
156. Ge L, Zuo M, Wang Y, et al. (2024) A review of comprehensive utilization of biomass to synthesize carbon nanotubes: From chemical vapor deposition to microwave pyrolysis. *J Anal Appl Pyrolysis* 177: 106320. https://doi.org/10.1016/j.jaap.2023.106320
157. Zhou G, Wu H, Deng Y, et al. (2024) Synthesis of high-quality multi-walled carbon nanotubes by arc discharge in nitrogen atmosphere. *Vacuum* 225: 113198. https://doi.org/10.1016/j.vacuum.2024.113198
158. Lv E, Miao W, Cheng M, et al. (2024) Synthesis of NbC@C(Nx) nanoparticles using DC arc discharge plasma for highly efficient oxygen reduction reaction. *Diam Relat.Mater* 144: 111010. https://doi.org/10.1016/j.diamond.2024.111040
159. Madhurima VP, Kumari K, Jain PK (2024) Synthesis and study of carbon nanomaterials through arc discharge technique for efficient adsorption of organic dyes. *Diam Relat Mater* 141:110538. https://doi.org/10.1016/j.diamond.2023.110538
160. Avinash K, Patolsky F (2023) Laser-induced graphene structures: From synthesis and applications to future prospects. *Materials Today* 70: 104–136. https://doi.org/10.1016/j.mattod.2023.10.009
161. Li Z, Wei X, Yang Z (2023) Pulsed laser 3D-micro/nanostructuring of materials for electrochemical energy storage and conversion. *Prog Mater Sci* 133: 101052. https://doi.org/10.1016/j.pmatsci.2022.101052

162. Fromme T, Reichenberger S, Tibbetts KM, et al. (2024) Laser synthesis of nanoparticles in organic solvents – products, reactions, and perspectives. *Beilstein J Nanotechnol* 15: 638–663. https://doi.org/10.3762/bjnano.15.54
163. Ismail RA, Mohsin MH, Ali AK, et al. (2020) Preparation and characterization of carbon nanotubes by pulsed laser ablation in water for optoelectronic application. *Physica E Low Dimens Syst Nanostruct* 119: 113997. https://doi.org/10.1016/j.physe.2020.113997
164. Chrzanowska J, Hoffman J, Małolepszy A, et al. (2015) Synthesis of carbon nanotubes by the laser ablation method: Effect of laser wavelength. *Phys Status Solidi* 252: 1860–1867. https://doi.org/10.1002/pssb.201451614
165. Mane P V, Rego RM, Yap PL, et al. (2024) Unveiling cutting-edge advances in high surface area porous materials for the efficient removal of toxic metal ions from water. *Prog Mater Sci* 146: 101314. https://doi.org/10.1016/j.pmatsci.2024.101314
166. Pervez MN, Jiang T, Mahato JK, et al. (2024) Surface Modification of Graphene Oxide for Fast Removal of Per- and Polyfluoroalkyl Substances (PFAS) Mixtures from River Water. *ACS ES T Water* 4: 2968–2980. https://doi.org/10.1021/acsestwater.4c00187
167. Tunioli F, Marforio TD, Favaretto L, et al. (2023) Chemical Tailoring of β-Cyclodextrin-Graphene Oxide for Enhanced Per- and Polyfluoroalkyl Substances (PFAS) Adsorption from Drinking Water. *Chem A Eur J* 29: e202301854. https://doi.org/10.1002/chem.202301854
168. Abidli A, Ben Rejeb Z, Zaoui A, et al. (2025) Comprehensive insights into the application of graphene-based aerogels for metals removal from aqueous media: Surface chemistry, mechanisms, and key features. *Adv Colloid Interface Sci* 335: 103338. https://doi.org/10.1016/j.cis.2024.103338
169. Mahpishanian S, Zhou M, Foudazi R (2024) Magnetic amino-functionalized graphene oxide nanocomposite for PFAS removal from water. *Environ Sci Adv*. https://doi.org/10.1039/D4VA00171K
170. Lin H, Buerki-Thurnherr T, Kaur J, Wick, et al. (2024) Environmental and Health Impacts of Graphene and Other Two-Dimensional Materials: A Graphene Flagship Perspective. *ACS Nano* 18: 6038–6094. https://doi.org/10.1021/acsnano.3c09699
171. Lin Y, Zhang Y, Li J, et al. (2020) Blood exposure to graphene oxide may cause anaphylactic death in non-human primates. *Nano Today* 35: 100922. https://doi.org/10.1016/j.nantod.2020.100922
172. Ou L, Song B, Liang H, et al. (2016) Toxicity of graphene-family nanoparticles: A general review of the origins and mechanisms. *Part Fibre Toxicol* 13: 57. https://doi.org/10.1186/s12989-016-0168-y
173. Liu J, Chen S, Liu Y, et al. (2022) Progress in preparation, characterization, surface functional modification of graphene oxide: A review. *J Saudi Chem Soc* 26. https://doi.org/10.1016/j.jscs.2022.101560
174. Zhang Q, Yang Y, Fan H, et al. (2022) Synthesis of graphene oxide using boric acid in hummers method. *Colloids Surf A Physicochem Eng Asp* 652: 129802. https://doi.org/10.1016/j.colsurfa.2022.129802
175. Marcano DC, Kosynkin D V, Berlin JM, et al. (2010) Improved synthesis of graphene oxide. *ACS Nano* 4: 4806–4814. https://doi.org/10.1021/nn1006368
176. Vatankhah H, Riley SM, Murray C, et al. (2019) Simultaneous ozone and granular activated carbon for advanced treatment of micropollutants in municipal wastewater effluent. *Chemosphere* 234: 845–854. https://doi.org/10.1016/j.chemosphere.2019.06.082

177. Podder MS, Majumder CB (2015) Removal of arsenic by a Bacillus arsenicus biofilm supported on GAC/MnFe2O4 composite. *Groundw Sustain Dev* 1: 105–128. https://doi.org/10.1016/j.gsd.2015.11.002
178. Moore BC, Cannon FS, Westrick JA, et al. (2001) Changes in GAC pore structure during full-scale water treatment at Cincinnati: A comparison between virgin and thermally reactivated GAC. *Carbon N Y* 39: 789–807. https://doi.org/10.1016/S0008-6223(00)00097-X
179. Sadia M, Beut LB, Pranić M, et al. (2024) Sorption of per- and poly-fluoroalkyl substances and their precursors on activated carbon under realistic drinking water conditions: Insights into sorbent variability and PFAS structural effects. *Heliyon* 10: e25130. https://doi.org/10.1016/j.heliyon.2024.e25130
180. Jjagwe J, Olupot PW, Menya E, et al. (2021) Synthesis and Application of Granular Activated Carbon from Biomass Waste Materials for Water Treatment: A Review. *J Bioresour Bioprod* 6: 292–322. https://doi.org/10.1016/j.jobab.2021.03.003
181. Liang C, Lee PH (2012) Granular activated carbon/pyrite composites for environmental application: Synthesis and characterization. *J Hazard Mater* 231–232: 120–126. https://doi.org/10.1016/j.jhazmat.2012.06.048
182. He Y, Cheng X, Gunjal SJ, et al. (2024) Advancing PFAS Sorbent Design: Mechanisms, Challenges, and Perspectives. *ACS Materials Au* 4: 108–114. https://doi.org/10.1021/acsmaterialsau.3c00066
183. Kim G, Mengesha DN, Choi Y (2024) Adsorption dynamics of per- and polyfluoroalkyl substances (PFAS) on activated carbon: Interplay of surface chemistry and PFAS structural properties. *Sep Purif Technol* 349: 127851. https://doi.org/10.1016/j.seppur.2024.127851
184. He Y, Cheng X, Gunjal SJ, et al. (2024) Advancing PFAS Sorbent Design: Mechanisms, Challenges, and Perspectives. *ACS Materials Au* 4: 108–114. https://doi.org/10.1021/acsmaterialsau.3c00066
185. Umeh AC, Hassan M, Egbuatu M, et al. (2023) Multicomponent PFAS sorption and desorption in common commercial adsorbents: Kinetics, isotherm, adsorbent dose, pH, and index ion and ionic strength effects. *Sci Total Environ* 904. https://doi.org/10.1016/j.scitotenv.2023.166568
186. Latour RA (2015) The Langmuir isotherm: A commonly applied but misleading approach for the analysis of protein adsorption behavior. *J Biomed Mater Res A* 103: 949–958. https://doi.org/10.1002/jbm.a.35235
187. Nishimura T, de Barros IR, Benincá C, et al. (2025) Inner-sphere adsorption of orthophosphates on amorphous aluminum hydroxide: The Laplace transform solution to a kinetic model involving first-order Taylor approximations to the Langmuir isotherm. *Sep Purif Technol* 369: 133086. https://doi.org/10.1016/j.seppur.2025.133086
188. Yang M, He X, Xu J, et al. (2024) Simplified approach to retention times of narrow binary pulses in the case of ideal chromatography model and Langmuir isotherm. *J Chromatogr A* 1736: 465405. https://doi.org/10.1016/j.chroma.2024.465405
189. Patiha Heraldy E, Hidayat Y, Firdaus M (2016) The langmuir isotherm adsorption equation: The monolayer approach. *IOP Conf Ser Mater Sci Eng* 107: 012067. https://doi.org/10.1088/1757-899X/107/1/012067
190. Marković VL, Stamenković SN (2025) Freundlich adsorption isotherm for description of gas – surface interaction. *Vacuum* 234: 114092. https://doi.org/10.1016/j.vacuum.2025.114092

191. Xu MX, Zhu HY, Miao T, et al. (2025) Statistical interpretation of Langmuir-Freundlich equation for physical adsorption by exchange-electron number of adsorbate with surface. *Sep Purif Technol* 373: 133501. https://doi.org/10.1016/j.seppur.2025.133501
192. Deivayanai VC, Karishma S, Thamarai P, et al. (2025) Advanced modeling of Congo red dye adsorption using magnetic nanoparticles functionalized with jackfruit seed waste biomass: A contemporary modeling approach. *Mater Chem Phys* 341: 130947. https://doi.org/10.1016/j.matchemphys.2025.130947
193. Mustapha S, Shuaib DT, Ndamitso MM, et al. (2019) Adsorption isotherm, kinetic and thermodynamic studies for the removal of Pb(II), Cd(II), Zn(II) and Cu(II) ions from aqueous solutions using Albizia lebbeck pods. *Appl. Water Sci* 9: 142. https://doi.org/10.1007/s13201-019-1021-x
194. Wang J, Guo X (2020) Adsorption kinetic models: Physical meanings, applications, and solving methods. *J Hazard Mater* 390: 122156. https://doi.org/10.1016/j.jhazmat.2020.122156
195. Khamwichit A, Dechapanya W, Dechapanya W (2022) Adsorption kinetics and isotherms of binary metal ion aqueous solution using untreated venus shell. *Heliyon* 8. https://doi.org/10.2139/ssrn.4037406
196. Al-Harby NF, Albahly EF, Mohamed NA (2021) Kinetics, Isotherm and Thermodynamic Studies for Efficient Adsorption of Congo Red Dye from Aqueous Solution onto Novel Cyanoguanidine-Modified Chitosan Adsorbent. *Polymers* 13: 4446. https://doi.org/10.3390/polym13244446
197. Sangoremi AA (2025) Adsorption Kinetic Models and Their Applications: A Critical Review. *Int J Res Sci Innov* 5: 245–258. https://doi.org/10.51244/IJRSI.2025.120500019
198. Hubbe M, Azizian S, Douven S (2019) Implications of apparent pseudo-second-order adsorption kinetics onto cellulosic materials: A review. *Bioresour* 14: 7582–7626. https://doi.org/10.15376/biores.14.3.Hubbe
199. Li X, Shen H, Pan X, et al. (2025) Kinetic study of the fluoride removal by gypsum using revised pseudo-second-order model: Insights on the surface adsorption and precipitation. *Surf Interfaces* 62. https://doi.org/10.1016/j.surfin.2025.106304
200. Dal MC, Onursal N (2023) Two new linearized equations derived from a pseudo-second-order kinetic model. *Desalin Water Treat* 308: 183–189. https://doi.org/10.5004/dwt.2023.29992
201. Park N, Kho Y, Kim J (2021) Levels of Perfluorinated Compounds in Liquid Milk Products in Korea. *J Food Hyg Saf* 36: 310–315. https://doi.org/10.13103/JFHS.2021.36.4.310
202. Welchert J, Dunmyer M, Carroll L, et al. (2024) Investigation into the adhesion properties of PFAS on model surfaces. *RSC Appl Interfaces* 1: 1265–1275. https://doi.org/10.1039/D4LF00228H
203. Tian Y, Zhou Q, Zhang L, et al. (2023) In utero exposure to per-/polyfluoroalkyl substances (PFASs): Preeclampsia in pregnancy and low birth weight for neonates. *Chemosphere* 313: 137490. https://doi.org/10.1016/j.chemosphere.2022.137490
204. Lim S, Kim JH, Park H, et al. (2021) Role of electrostatic interactions in the adsorption of dye molecules by Ti 3 C 2 -MXenes. *RSC Adv* 11: 6201–6211. https://doi.org/10.1039/D0RA10876F
205. Nasrollahpour S, Pulicharla R, Brar SK (2025) Functionalized biochar for the removal of poly- and perfluoroalkyl substances in aqueous media. *iScience* 28: 112113. https://doi.org/10.1016/j.isci.2025.112113

206. Behroozi AH, Meunier L, Mirahsani A, et al. (2025) Graphene-based materials and technologies for the treatment of PFAS in water: A review of recent developments. *J Hazard Mater Adv* 17: 100626. https://doi.org/10.1016/j.hazadv.2025.100626
207. Bagotia N, Choudhary V, Sharma DK (2019) Synergistic effect of graphene/multiwalled carbon nanotube hybrid fillers on mechanical, electrical and EMI shielding properties of polycarbonate/ethylene methyl acrylate nanocomposites. *Compos B Eng* 159: 378–388. https://doi.org/10.1016/j.compositesb.2018.10.009
208. Zhu J, Wen W, Tian Z, et al. (2023) Covalent organic framework: A state-of-the-art review of electrochemical sensing applications. *Talanta* 260. https://doi.org/10.1016/j.talanta.2023.124613
209. Jain M, Sahoo A, Mishra D, et al. (2024) Modelling and statistical interpretation of phenol adsorption behaviour of 3-Dimensional hybrid aerogel of waste-derived carbon nanotubes and graphene oxide. *Chem Eng J* 490: 151351. https://doi.org/10.1016/j.cej.2024.151351
210. Tay MF, Liu C, Cornelissen ER, et al. (2018) The feasibility of nanofiltration membrane bioreactor (NF-MBR)+reverse osmosis (RO) process for water reclamation: Comparison with ultrafiltration membrane bioreactor (UF-MBR)+RO process. *Water Res* 129: 180–189. https://doi.org/10.1016/j.watres.2017.11.013
211. Dolar D, Košutić K (2013) Removal of pharmaceuticals by ultrafiltration (UF), nanofiltration (NF), and reverse osmosis (RO). *Compr Anal Chem* 62: 319–344. https://doi.org/10.1016/B978-0-444-62657-8.00010-0
212. Elfilali N, Elazhar F, Dhiba D, et al. (2022) Performances of various hybrids systems coagulation–ultrafiltration/ nanofiltration-reverse osmosis in the treatment of stabilized landfill leachate. *Desalin Water Treat* 257: 55–63. https://doi.org/10.5004/dwt.2022.28360
213. Issaka E, AMU-Darko JNO, Yakubu S, et al. (2022) Advanced catalytic ozonation for degradation of pharmaceutical pollutants—A review. *Chemosphere* 289: 133208. https://doi.org/10.1016/j.chemosphere.2021.133208
214. Issaka E, Danso-Boateng E, Baffoe J (2024) Harnessing the Power of Heterogeneous Photocatalytic Process for Sustainable Pharmaceutical Contaminant Remediation in Water Environments. *Desalin Water Treat* 319: 100574. https://doi.org/10.1016/j.dwt.2024.100574
215. Issaka E, Adams M, El-Ouardy S, et al. (2025) Photoelectrochemical alchemy: Transforming wastewater pollutants through photoelectrochemical advanced oxidation processes. *Desalin Water Treat* 321: 101057. https://doi.org/10.1016/j.dwt.2025.101057
216. Issaka E (2024) From Complex Molecules to Harmless Byproducts: Electrocoagulation Process for Water Contaminants Degradation. *Desalin Water Treat* 100532. https://doi.org/10.1016/j.dwt.2024.100532
217. Rekik H, Arab H, Pichon L, et al. (2024) Per-and polyfluoroalkyl (PFAS) eternal pollutants: Sources, environmental impacts and treatment processes. *Chemosphere* 358: 142044. https://doi.org/10.1016/j.chemosphere.2024.142044
218. Dai Y, Niu J, Yin L, et al. (2013) Enhanced sorption of perfluorooctane sulfonate (PFOS) on carbon nanotube-filled electrospun nanofibrous membranes. *Chemosphere* 93: 1593–1599. https://doi.org/10.1016/j.chemosphere.2013.08.013
219. Zhou Y, Wen B, Pei Z, et al. (2012) Coadsorption of copper and perfluorooctane sulfonate onto multi-walled carbon nanotubes. *Chem Eng J* 203: 148–157. https://doi.org/10.1016/j.cej.2012.06.156

220. Kwadijk CJAF, Velzeboer I, Koelmans AA (2013) Sorption of perfluorooctane sulfonate to carbon nanotubes in aquatic sediments. *Chemosphere* 90: 1631–1636. https://doi.org/10.1016/j.chemosphere.2012.08.041
221. Deng S, Zhang Q, Nie Y, et al. (2012) Sorption mechanisms of perfluorinated compounds on carbon nanotubes. *Environ Pollut* 168: 138–144. https://doi.org/10.1016/j.envpol.2012.03.048
222. Bei Y, Deng S, Du Z, et al. (2014) Adsorption of perfluorooctane sulfonate on carbon nanotubes: Influence of pH and competitive ions. *Water Sci Technol* 6: 1489–1495. https://doi.org/10.2166/wst.2014.049
223. Chen X, Xia X, Wang X, et al.. (2011) A comparative study on sorption of perfluorooctane sulfonate (PFOS) by chars, ash and carbon nanotubes. *Chemosphere* 83: 1313–1319. https://doi.org/10.1016/j.chemosphere.2011.04.018
224. Azmi LHM, Williams DR, Ladewig BP (2020) Polymer-Assisted Modification of Metal-Organic Framework MIL-96 (Al): Influence on Particle Size, Crystal Morphology and Perfluorooctanoic Acid (PFOA) Removal. *Chem* 1.
225. Hassan M, Liu Y, Naidu R, et al. (2020) Adsorption of Perfluorooctane sulfonate (PFOS) onto metal oxides modified biochar. *Environ Technol Innov* 19: 100816. https://doi.org/10.1016/j.eti.2020.100816
226. Li R, Alomari S, Stanton R, et al. (2021) Efficient Removal of Per- and Polyfluoroalkyl Substances from Water with Zirconium-Based Metal–Organic Frameworks. *Chem Mat* 33: 3276–3285. https://doi.org/10.1021/acs.chemmater.1c00324
227. Xing DY, Chen Y, Zhu J, et al. (2020) Fabrication of hydrolytically stable magnetic core-shell aminosilane nanocomposite for the adsorption of PFOS and PFOA. *Chemosphere* 251: 126384. https://doi.org/10.1016/j.chemosphere.2020.126384
228. Xu J, Liu Z, Zhao D, et al. (2020) Enhanced adsorption of perfluorooctanoic acid (PFOA) from water by granular activated carbon supported magnetite nanoparticles. *Sci Total Environ* 723: 137757. https://doi.org/10.1016/j.scitotenv.2020.137757
229. Yuan J, Mortazavian S, Passeport E, et al. (2022) Evaluating perfluorooctanoic acid (PFOA) and perfluorooctanesulfonic acid (PFOS) removal across granular activated carbon (GAC) filter-adsorbers in drinking water treatment plants. *Sci Total Environ* 838: 156406. https://doi.org/10.1016/j.scitotenv.2022.156406
230. Wang M, Rivenbark KJ, Nikkhah H, et al. (2024) In vitro and in vivo remediation of per- and polyfluoroalkyl substances by processed and amended clays and activated carbon in soil. *Applied Soil Ecology* 196: 105285. https://doi.org/10.1016/j.apsoil.2024.105285
231. Molé RA, Velosa AC, Carey GR, et al. (2024) Groundwater solutes influence the adsorption of short-chain perfluoroalkyl acids (PFAA) to colloidal activated carbon and impact performance for in situ groundwater remediation. *J Hazard Mater* 474: 134746. https://doi.org/10.1016/j.jhazmat.2024.134746
232. Abou-Khalil C, Kewalramani J, Zhang Z, et al. (2023) Effect of clay content on the mobilization efficiency of per- and polyfluoroalkyl substances (PFAS) from soils by electrokinetics and hydraulic flushing. *Environ Pollut* 322: 121160. https://doi.org/10.1016/j.envpol.2023.121160
233. Pervez MN, Jiang T, Mahato JK, et al. (2024) Surface Modification of Graphene Oxide for Fast Removal of Per- and Polyfluoroalkyl Substances (PFAS) Mixtures from River Water. *ACS ES T Water* 4: 2968–2980. https://doi.org/10.1021/acsestwater.4c00187

234. Satyam S, Patra S (2024) Innovations and challenges in adsorption-based wastewater remediation: A comprehensive review. *Heliyon* 10: e29573. https://doi.org/10.1016/j.heliyon.2024.e29573
235. Han H, Khalid Rafiq M, Zhou T, et al. (2019) A critical review of clay-based composites with enhanced adsorption performance for metal and organic pollutants. https://doi.org/10.1016/j.jhazmat.2019.02.003
236. Murray CC, Marshall RE, Liu CJ, et al. (2021) PFAS treatment with granular activated carbon and ion exchange resin: Comparing chain length, empty bed contact time, and cost. *Environ Pollut* 44: 102342. https://doi.org/10.1016/j.jwpe.2021.102342
237. Duchesne AL, Brown JK, Patch DJ, et al. (2020) Remediation of PFAS-Contaminated Soil and Granular Activated Carbon by Smoldering Combustion. *Environ Sci Technol* 54: 12631–12640. https://doi.org/10.1021/acs.est.0c03058
238. McCleaf P, Englund S, Östlund A, et al. (2017) Removal efficiency of multiple poly- and perfluoroalkyl substances (PFASs) in drinking water using granular activated carbon (GAC) and anion exchange (AE) column tests. *Water Res* 120: 77–87. https://doi.org/10.1016/j.watres.2017.04.057
239. Han H, Khalid Rafiq M, Zhou T, et al. (2019) A critical review of clay-based composites with enhanced adsorption performance for metal and organic pollutants. https://doi.org/10.1016/j.jhazmat.2019.02.003
240. Chomba C, Abdalqadir M, Gomari SR (2022) Investigation of different clay activation techniques to capture and store carbon dioxide (CO2).
241. Gul Zaman H, Baloo L, Pendyala R, et al. (2021) Produced Water Treatment with Conventional Adsorbents and MOF as an Alternative: A Review. *Materials* 14: 7607. https://doi.org/10.3390/ma14247607
242. Ramanayaka S, Vithanage M, Sarmah A, et al. (2019) Performance of metal–organic frameworks for the adsorptive removal of potentially toxic elements in a water system: a critical review. *RSC Adv* 9: 34359–34376. https://doi.org/10.1039/C9RA06879A
243. Aprilio K, Sari AP, Putri AMH, et al. (2023) Synthesis and Characterization of MOFs/Activated Carbon composite on Carbon-Dioxide Adsorption. *AIP Conf Proc* 2902. https://doi.org/10.1063/5.0173145
244. Alyasi H, Wahib S, Gomez TA, et al. (2024) The power of MXene-based materials for emerging contaminant removal from water - A review. *Desalination* 586: 117913. https://doi.org/10.1016/j.desal.2024.117913
245. Mo F, Zhou Q, Wang Q, et al. (2022) The applications of MOFs related materials in photo/electrochemical decontamination: An updated review. *Chem Eng J* 450: 138326. https://doi.org/10.1016/j.cej.2022.138326
246. Padhye LP, Srivastava P, Jasemizad T, et al. (2023) Contaminant containment for sustainable remediation of persistent contaminants in soil and groundwater. *J Hazard Mater* 455: 131575. https://doi.org/10.1016/j.jhazmat.2023.131575
247. Liu F, Pignatello JJ, Sun R, et al. (2024) A Comprehensive Review of Novel Adsorbents for Per- and Polyfluoroalkyl Substances in Water. *ACS ES&T Water* 4: 1191–1205 https://doi.org/10.1021/acsestwater.3c00569
248. Bresnahan CG, Schutt TC, Shukla MK (2023) Exploration of functionalizing graphene and the subsequent impact on PFAS adsorption capabilities via molecular dynamics. *Chemosphere* 345: 140462. https://doi.org/10.1016/j.chemosphere.2023.140462

249. Issaka E, Amu-Darko JNO, Adams M, et al. (2023) Zinc Imidazolate Metal–Organic Frameworks-8-Encapsulated Enzymes/Nanoenzymes for Biocatalytic and Biomedical Applications. *Catal. Letters* 153: 2083–2106. https://doi.org/10.1007/s10562-022-04140-x
250. Labine LM, Oliveira Pereira EA, Kleywegt S, et al. (2022) Comparison of sub-lethal metabolic perturbations of select legacy and novel perfluorinated alkyl substances (PFAS) in Daphnia magna. *Environ Res* 212: 113582. https://doi.org/10.1016/j.envres.2022.113582
251. Saleh N, Khalid A, Tian Y (2019) Removal of poly-and per-fluoroalkyl substances from aqueous systems by nano-enabled water treatment strategies. *Environ Pollut Res* 5: 198-208. https://doi.org/10.1039/C8EW00621K
252. Zhang W, Zhang D, Liang Y (2019) Nanotechnology in remediation of water contaminated by poly-and perfluoroalkyl substances: A review. *Environ Pollut* 247: 266-276. https://doi.org/10.1016/j.envpol.2019.01.045
253. Lawrence JR, Waiser MJ, Swerhone GDW, et al. (2016) Effects of fullerene (C60), multi-wall carbon nanotubes (MWCNT), single wall carbon nanotubes (SWCNT) and hydroxyl and carboxyl modified single wall carbon nanotubes on riverine microbial communities. *Environ Sci Pollut Res* 23: 10090–10102. https://doi.org/10.1007/s11356-016-6244-x
254. Shafi A, Khan N, Sultana S, et al. (2021) Nanoremediation technologies for sustainable remediation of contaminated environments: Recent advances and challenges. *Chemosphere* 275: 130065.
255. Oyetade OA, Varadwaj GBB, Nyamori VO, et al. (2018) A critical review of the occurrence of perfluoroalkyl acids in aqueous environments and their removal by adsorption onto carbon nanotubes. *Rev Environ Sci Biotechnol* 17: 603–635. https://doi.org/10.1007/s11157-018-9479-9
256. Yin S, Villagrán D (2022) Design of nanomaterials for the removal of per- and poly-fluoroalkyl substances (PFAS) in water: Strategies, mechanisms, challenges, and opportunities. *Sci Total Environ* 831: 154939. https://doi.org/10.1016/j.scitotenv.2022.154939
257. Zhou Y, Wen B, Pei Z, et al. (2012) Coadsorption of copper and perfluorooctane sulfonate onto multi-walled carbon nanotubes. *Chem Eng J* 203: 148–157. https://doi.org/10.1016/j.cej.2012.06.156
258. Lei X, Yao L, Lian Q, et al.. (2022) Enhanced adsorption of perfluorooctanoate (PFOA) onto low oxygen content ordered mesoporous carbon (OMC): Adsorption behaviors and mechanisms. *J Hazard Mater* 421: 126810. https://doi.org/10.1016/j.jhazmat.2021.126810
259. Issaka E, Danso-Boateng E, Fazal A, et al. (2025) Algae biomass for energy generation: a comprehensive review of recent advances, mechanisms and bottlenecks. *Sustain Green Mater* 1: 32-94. https://doi.org/10.1080/29965292.2025.2515823
260. Jansson S, Boman C, Lindgren R, et al. (2022) Activated and non-activated biochars and hydrochars from forestry-related waste streams for removal of environmental contaminants from sediments. *BIO4ENERGY*.
261. Neha S, Nguyen M, Vergeynst L, et al. (2025) PFAS destruction through catalyzed hydrothermal liquefaction using modified hydrochar. *Environ Pollut* 72: 107606. https://doi.org/10.1016/j.jwpe.2025.107606
262. Liang D, Li C, Chen H, et al. (2024) A critical review of biochar for the remediation of PFAS-contaminated soil and water. *Sci Total Environ* 951: 174962. https://doi.org/10.1016/j.scitotenv.2024.174962

263. Niaz W, Zhang D, Ahmad Z, et al. (2024) Efficient removal of perfluorooctanoic acid (PFOA) and perfluorooctane sulfonic acid (PFOS) from aqueous solution using modified biochar: Preparation, performance, and mechanistic insights. *J Environ Chem Eng* 12: 114894. https://doi.org/10.1016/j.jece.2024.114894
264. Biochar Today (2024) Biochar-Based Adsorbents Show Promise for PFAS Removal in Water Treatment.
265. Cheng J, Islam MT, Sadmani AHMA, et al. (2024) The effect of biochar in a specialty adsorbent on enhanced PFAS removal from surface water. *Environ Pollut* 67: 106231. https://doi.org/10.1016/j.jwpe.2024.106231
266. Chen W, Cannon FS, Rangel-Mendez JR (2005) Ammonia-tailoring of GAC to enhance perchlorate removal. I: Characterization of NH3 thermally tailored GACs. *Carbon N Y* 43: 573–580. https://doi.org/10.1016/j.carbon.2004.10.024
267. Seider V, Gallardo-Bustos C, Vargas IT (2025) Multidimensional assessment of (bio)electrochemical GAC-packed bed filters for laundry greywater treatment. *Environ Pollut* 77: 108514. https://doi.org/10.1016/j.jwpe.2025.108514
268. Li X, Yu G, Noman M, et al. (2025) Biochar derived from synergistic co-pyrolysis of digestate residue and polyvinyl chloride for efficient ammonia adsorption: behaviors, characterizations, and mechanisms. *J Indian Chem Soc* 102: 101996. https://doi.org/10.1016/j.jics.2025.101996
269. Moore BC, Cannon FS, Westrick JA, et al. (2001) Changes in GAC pore structure during full-scale water treatment at Cincinnati: a comparison between virgin and thermally reactivated GAC. *Carbon N Y* 39: 789–807. https://doi.org/10.1016/S0008-6223(00)00097-X
270. Wang J, Lin Z, He X, et al. (2022) Critical Review of Thermal Decomposition of Per- and Polyfluoroalkyl Substances: Mechanisms and Implications for Thermal Treatment Processes. *Environ Sci Technol* 56: 5355–5370. https://doi.org/10.1021/acs.est.2c02251
271. An K, Li K, Yang CM, et al. (2023) A comprehensive review on regeneration strategies for direct air capture. *J CO_2 Util* 76: 102587. https://doi.org/10.1016/j.jcou.2023.102587
272. Assad H, Lone IA, Kumar A, et al. (2024) Unveiling the contemporary progress of graphene-based nanomaterials with a particular focus on the removal of contaminants from water: a comprehensive review. *Front Chem* 12: 1347129. https://doi.org/10.3389/fchem.2024.1347129
273. Hassan MA, Al-Shemy MT, Kamal KH, et al. (2025) Hydrogel-activated hydrochar synergy for efficient wastewater purification: tackling imidacloprid pesticides and crystal violet dye. *Appl Water Sci* 15: 197. https://doi.org/10.1007/s13201-025-02553-8
274. Pinkard BR, Austin C, Purohit AL, et al. (2023) Destruction of PFAS in AFFF-impacted fire training pit water, with a continuous hydrothermal alkaline treatment reactor. *Chemosphere* 314: 137681. https://doi.org/10.1016/j.chemosphere.2022.137681
275. Sheng Y, Zhou Y, Tang C, et al. (2022) Redispersible Reduced Graphene Oxide Prepared in a Gradient Solvent System. *Nanomaterials* 12: 1982. https://doi.org/10.3390/nano12121982
276. Tshangana CS, Nhlengethwa ST, Glass S, et al. (2025) Technology status to treat PFAS-contaminated water and limiting factors for their effective full-scale application. *npj Clean Water* 8: 1–30. https://doi.org/10.1038/s41545-025-00457-3
277. Chang PH, Yang Y, Wen Y, et al. (2024) Efficient ethidium bromide removal using sodium alginate/graphene oxide composite beads: Insights into adsorption mechanisms and performance. *Chem Eng J* 500. https://doi.org/10.1016/j.cej.2024.156379

278. Raut S, Sahoo JK, Sahoo SK (2025) Electrospun MXene based functionalized nanofibers for water pollutants adsorption: Potentials, challenges and future perspective. *J Mol Liq* 433. https://doi.org/10.1016/j.molliq.2025.127871
279. El-Shamy OAA, Siddiqui MR, Mele G, et al. (2025) Synthesis, characterization and application of CNTs@Co-MOF and FCNTs@Co-MOF as superior supercapacitor: Experimental and theoretical studies. *J Mol Struct* 1321: 140161. https://doi.org/10.1016/j.molstruc.2024.140161

AIMS Press